

https://dspace.org/

Effect of gold nanoparticles on the activity of perovskites for CO oxidation

Mokoena, Lebohang Vivacious

2011-11-18
http://hdl.handle.net/10539/10809

Downloaded from a DSpace repository. https://dspace.org/

Effect of gold nanoparticles on the activity of perovskites for CO oxidation

Molecular Science Institute
School of Chemistry
University of the Witwatersrand, Johannesburg,
Private Bag, X3, P.O. WITS 2050,
SOUTH AFRICA.

TITLE

Effect of gold nanoparticles on the activity of perovskites for CO oxidation

By

Lebohang Vivacious Mokoena

"A dissertation submitted to the Faculty of Science, University of the Witwatersrand, Johannesburg, in fulfilment of the requirements for the degree of Master of science."

Johannesburg, 2011.

DECLARATION

I, _____Lebohang Vivacious Mokoena_____

declare that this is my own, unaided work. It is being submitted for the degree of Masters of Science in the University of the Witwatersrand, Gauteng. It has not been submitted before for any degree or examination in any other University.



_____

Signature of Candidate

____17th___ Day of June 2011

ABSTRACT

Gold has for many years been regarded as being inert and catalytically inactive compared to the PGMs (platinum group metals). However, in the past decade it has attracted a lot of interest as both a heterogeneous and a homogenous catalyst and has been shown to catalyse a wide range of reactions e.g. oxidation, hydrogenation and reduction among others. Highly dispersed gold nanoparticles on metal oxides, like titanium oxide (Degussa, P25) have predominantly been studied because they yield some of the most active and stable catalysts. Modification of the catalysts and/or supports has been shown to affect their catalytic properties.

Likewise, perovskites, which can be manipulated by partial substitution, are reported to be active supports for CO oxidation, but only at high temperatures with no activity shown for temperatures below 200°C. In this study, these perovskites were investigated at low temperatures (below 100°C) with improved activity found upon gold deposition. The presence of gold nanoparticles therefore significantly enhanced the catalytic activity, while the support itself was suspected to be involved in the reaction mechanism.

A series of perovskites of the type ABO_3 ($LaMnO_3$, $LaFeO_3$, $LaCoO_3$ and $LaCuO_3$) were prepared using the citrate method, while the gold was deposited on them using the deposition-precipitation method. The supports were calcined at different temperatures for optimisation. The catalysts were tested for carbon monoxide oxidation and the active catalysts characterised by XRF, XPS, XRD, Raman spectroscopy and BET surface area measurements.

With the support calcined at 800ºC, the best catalyst was then modified and compared with the unmodified catalyst. The 1-wt%Au supported on $LaFeO_3$ was found to give the best catalytic performance. This support was then modified with various weight loadings of calcium to determine the effect of calcium on the catalytic activity.

Calcium-doped materials showed decreased surface area, poorer crystallinity and a drop in catalytic activity relative to the Au-$LaFeO_3$ which indicated the best results for CO oxidation. In addition, Au-$LaFeO_3$ showed online stability over 21 hours.

Calcining the support improved the incorporation of gold nanoparticles into the perovskite lattice, resulting in superior catalytic activity. Nevertheless, at higher calcination temperatures, the catalytic activity of Au-$CaTiO_3$ was depressed while that of Au-$LaFeO_3$ was enhanced. The activity of perovskites increased upon gold deposition. XPS, revealed that in the active catalysts, both cationic and metallic gold co-existed, whilst in the inactive catalysts the gold existed predominantly either as cationic or metallic gold.

DEDICATION

In memory of my late grandmother

Thandiwe Jane Makhubo

ACKNOWLEDGEMENTS

I would like to express my deepest gratitude to the following people and institutions for the various roles in making this project a success:

- My supervisor, Prof. M. S. Scurrell, for his guidance and helpful suggestions during this project
- Basil Chassoulas for all his technical help
- Albert Carley from Cardiff University for the XPS analysis
- Werner Jordaan from NMISA for the TOF-SIMS analysis
- Rudolph Erasmus from the University of the Witwatersrand for the Raman spectroscopy analysis
- Performance Laboratories for the gold content analysis
- Sharon from the University of the Witwatersrand for the XRF analysis
- My main sponsor for the project, MINTEK, through project AuTEK, for the financial assistance
- NRF, South Africa, for additional funding
- The University of the Witwatersrand for allowing me to undertake this project
- My family, my mom, dad, sister, brother and my fiancé for their undying love and support
- The Catalysis, Organometallic and Materials (CATOMAT) group members of the School of Chemistry at the University of the Witwatersrand for providing a wonderful working environment and helpful suggestions
- Prof. L. Carlton from the University of the Witwatersrand for his guidance and belief in me
- All other friends who helped in one way or another
- Above all to God almighty

CONTENTS

Pages

TITLE II

DECLARATION III

ABSTRACT IV

DEDICATION VI

ACKNOWLEDGEMENTS VII

ABBREVIATIONS XIII

1 INTRODUCTION 1

1.1 Basic Principles of Catalysis 1
1.2 Classification of Catalytic Systems 3
1.3 Requirements for a Catalyst 5
1.4 History of Catalysis 6
1.5 References 7

2 GOLD IN CATALYSIS 8

2.1 Background 8
2.2 Properties, characteristics, uses and chemistry of gold 10
2.3 Gold as a Catalyst 13
2.4 Methods of preparing gold catalysts 15
2.4.1 Deposition–precipitation method [17] 16
2.4.2 Impregnation method [17] 17
2.4.3 Precipitation method [17] 17
2.4.4 Ion-exchange method [17] 17
2.4.5 Vapour-phase deposition and grafting method [17] 18
2.4.6 Co-sputtering method [17] 18
2.4.7 Colloidal mixing method [17] 18
2.4.8 Other methods 19
2.5 Characterisation of Gold Catalysts 19
2.5.1 Transmission Electron Microscopy (TEM) 19
2.5.2 Nitrogen physiosorption (BET surface area) 20
2.5.3 X-Ray Diffraction (XRD) 20
2.5.4 Inductively Coupled Plasma (ICP) Elemental Analysis 20
2.5.5 Photoelectron spectroscopy (X-Ray and UV-induced) 21
2.5.6 Infrared (IR) Spectroscopy 21
2.5.7 Extended X-ray absorption fine structure (EXAFS) 21
2.5.8 Mössbauer Spectroscopy 22

2.5.9 Other methods *22*
2.6 Summary 23
2.5 References 24

3 PEROVSKITES 26

3.1 Introduction 26
3.2 Properties, Uses and Characteristics of Perovskites 28
3.3 Oxidation Catalysis using Perovskites 29
3.5 Motivation of Study 34
3.5 Aims and Objectives 35
3.6 References 37

4 EXPERIMENTAL METHODS 38

4.1 Reagents 38
4.2 Preparation of Supports 39
4.2.1 Preparation of $CaTiO_3$ *39*
4.2.2 Preparation of $La_{1-x}Ca_xFeO_3$ *39*
4.3 Preparation of Au Catalysts 41
4.4 Activity Measurements 41
4.5 Characterization 43
4.5.1 BET surface area determination *43*
4.5.2 X-ray powder diffraction *43*
4.5.3 Raman spectroscopy *43*
4.5.4 X-ray photoelectron spectroscopy *44*
4.6 Calculations 44
4.7 References 45

5 CATALYSTS BASED ON CALCIUM-TITANIUM PEROVSKITES 46

5.1 Activity and Stability Measurements for Au-$CaTiO_3$ 47
5.1.1 Activity Tests *48*
5.1.2 Stability Tests *49*
5.2 Characterisation Results for Au-$CaTiO_3$ 51
5.2.1 BET surface area *52*
5.2.2 X-ray diffraction *53*
5.2.3 Raman spectroscopy *54*
5.2.4 X-ray photoelectron spectroscopy *55*
5.3 Discussion 58
5.4 References 60

6 CATALYSTS BASED ON LANTHANUM-IRON PEROVSKITES 61

6.1 Activity Measurements for Au-$LaFeO_3$ 61
6.1.1 Activity Tests *62*
6.1.2 Stability Tests *63*
6.2 Characterisation results for Au-$LaFeO_3$ 65
6.2.1 BET surface area *66*

6.2.2 X-ray diffraction *66*
6.2.3 Raman spectroscopy *67*
6.2.4 X-ray photoelectron spectroscopy *69*
6.3 Discussion 72
6.4 References 73
7 CATALYSTS ON SUBSTTUTED LANTHANUM-IRON PEROVSKITES 74
7.1 Activity Measurements for Au-$La_{1-x}Ca_xFeO_3$ 74
7.1.1 Activity Tests *75*
7.1.2 Stability tests *76*
7.2 Characterisation Results for Au-$La_{1-x}Ca_xFeO_3$ 78
7.2.1 BET surface area *79*
7.2.2 X-ray diffraction *79*
7.2.3 Raman Spectroscopy *80*
7.2.4 X- ray photoelectron spectroscopy *81*
7.3 Discussion 85
7.4 References 86
8 CONCLUSION 87

LIST OF FIGURES

Figure 1: Some physical properties of platinum, mercury and the metals of group II. 9
Figure 2: The general perovskite structure [1]. 27
Figure 3: $LaFeO_3$ after being heated at 100 ºC overnight 40
Figure 4: $La_{1-x}Ca_xFeO_3$ (x = 4%, 10%, 16% and 20%) after being heated at 100 ºC. 40
Figure 5: Schematic representation of a reactor used for CO oxidation. 42
Figure 6: CO conversion over Au-$CaTiO_3$ catalysts 49
Figure 7: Stability tests for Au-$CaTiO_3$ catalysts 51
Figure 8: Diffractograms for $CaTiO_3$ calcined at different temperatures 53
Figure 9: Raman spectra for $CaTiO_3$ calcined at different temperatures 55
Figure 10: Spectra showing Au (4f) binding energies for Au-$CaTiO_3$ 56
Figure 11: Spectra for Au-$CaTiO_3$ showing the Ca (2p) binding energies 57
Figure 12: The spectra showing the O (1s) binding energies for Au-$CaTiO_3$ 57
Figure 13: CO conversion over Au-$LaFeO_3$ catalysts 63
Figure 14: CO conversion for Au-$LaFeO_3$ catalysts 65
Figure 15: Diffractograms for $LaFeO_3$ systems at various calcination temperatures. 67
Figure 16: Raman spectra for $LaFeO_3$ at different calcination temperatures 69
Figure 17: Spectra showing Au (4f) binding energies for Au-$LaFeO_3$ 70
Figure 18: Spectra showing La (3d) binding energies for Au-$LaFeO_3$ 70
Figure 19: Spectra showing Fe (2p) binding energies for Au-$LaFeO_3$ 71
Figure 20: Spectra showing O (1s) binding energies for Au-$LaFeO_3$ 71
Figure 21: CO conversion over Au-$La_{1-x}Ca_xFeO_3$ at different reaction temperatures 76
Figure 22: CO conversion over time on stream for Au-$La_{1-x}Ca_xFeO_3$ 78
Figure 23: XRD patterns showing the effect of calcium loading on $LaFeO_3$ 80
Figure 24: Spectra showing Au (4f) binding energies for Ca doped Au-$LaFeO_3$ 82
Figure 25: Spectra showing Ca (2p) binding energies for Ca doped Au-$LaFeO_3$ 82
Figure 26: Spectra showing La (3d) binding energies for Ca doped Au-$LaFeO_3$ 83
Figure 27: Spectra showing Fe (2p) binding energies for Ca doped Au-$LaFeO_3$ 83
Figure 28: Spectra showing O (1s) binding energies for Ca doped Au-$LaFeO_3$ 84

LIST OF TABLES

Table 1: Number of phase combinations in heterogeneous systems [7] 3
Table 2: Classification of heterogeneous catalysts [7] 4
Table 3: Basic properties of gold [4] 10
Table 4: Other gold uses [4] 11
Table 5: Comparison of the properties of Au with Ag and Cu [4] 12
Table 6: Perovskite-type oxides as oxidation catalysts [6] 30
Table 7: Activity measurements for the different gold-supported perovskites 47
Table 8: Activity measurements for Au-$CaTiO_3$ catalysts 48
Table 9: Stability measurements for Au-$CaTiO_3$ catalysts 50
Table 10: BET Surface area results for $CaTiO_3$ calcined at different temperatures 52
Table 11: Symmetry assignments for the observed Raman spectra for $CaTiO_3$ 54
Table 12: Surface compositions for Au-$CaTiO_3$ by XPS 56
Table 13: Activity measurements for the Au-$LaFeO_3$ system 62
Table 14: Stability measurements for Au-$LaFeO_3$ catalysts 64
Table 15: Surface area analysis for $LaFeO_3$ calcined at different temperatures 66
Table 16: Symmetry assignments for observed Raman peaks for $LaFeO_3$ 68
Table 17: Activity measurements for Au-$La_{1-x}Ca_xFeO_3$ 75
Table 18: Stability measurements for Au-$La_{1-x}Ca_xFeO_3$ 77
Table 19: Surface area results for Au-$La_{1-x}Ca_xFeO_3$ 79

ABBREVIATIONS

BET	Brunauer Emmet and Teller
XRD	X-ray Diffraction
TEM	Transmission Electron Microscopy
XPS	X-ray Photoelectron Spectroscopy
XAS	X-ray Absorption Spectroscopy
IR	Infrared
UPS	UV-induced Photoelectron Spectroscopy
ICP	Inductively Coupled Plasma emission/absorption spectroscopy

CHAPTER 1

1 INTRODUCTION

Gold catalysts have been investigated extensively in order to understand the mechanism of their catalytic activity, especially in low temperature CO oxidation reactions. The Au-TiO_2 system has by far proved to be the most active catalyst, although it deactivates over time [1, 2]. Since the support plays an important role in catalyst activity and stability [3], in this project we have attempted to design a stable catalyst, by depositing gold nanoparticles on some titanium-containing materials, namely the perovskites. These have the formula ABO_3, where A and B are metal atoms. Perovskites can be manipulated by partial substitution of either the A or B site or both, in order to create structural defects. As a result, the activity and stability can be optimised [4, 5, 6].

In this Chapter, a brief background of general catalysis is given, including the basic principles, classification of catalytic systems and solid catalysts, requirements for catalysts and a brief history of catalysis from different sources as referenced.

1.1 Basic Principles of Catalysis

The word '**catalysis**' comes from two Greek words, with the prefix '*cata-*' meaning 'down' and the verb '*lysein'*, meaning 'to split or break'. A catalyst generally is defined as a substance that increases the rate at which a chemical system approaches its equilibrium without being consumed in the process.

Catalysis has made major contributions to many areas in the chemical industry. Most products are manufactured through catalysis and, importantly, many of the difficulties which we face today, such as problems of energy, natural resources, pollution etc, can be solved by catalysis [7]. Catalysis plays a vital role, not only in the removal of pollutants such as NO_x, CO and sulphur compounds, but also in improving the selectivity of manufacturing processes so that undesirable by-products are not generated [8]. Catalysis and catalyst development is essential in the production of a wide range of chemicals or products, such as wine, detergents, beer, fertilizers and herbicides which otherwise could not be obtained or would be very expensive to produce [8].

To understand the process of catalysis and to study a reacting chemical system, the following points need to be considered. Firstly, the extent to which the reaction will proceed, if it will proceed at all and the equilibrium position of the system. The answers to these and related questions are found in thermodynamics. Secondly, the rate of the reaction, i.e. how rapidly the equilibrium will be reached and other related questions are found by chemical kinetics. Both considerations are important in the design of a chemical process [7].

No matter how fast the reaction proceeds, the yield and equilibrium constant are both central to the process viability. For instance, a process with a very small equilibrium constant and a low yield of product will not normally be economically viable [7].

Essentially, a catalyst will only increase the rate of the reaction if the reaction is favourable thermodynamically. It cannot initiate a reaction that is not feasible. It does not alter the equilibrium constant as it only increases the rate of the forward and reverse reactions [7].

1.2 Classification of Catalytic Systems

Catalytic systems can be divided into two distinct categories [7]:

1. Homogenous: catalyst and reactants are of the same phase i.e. there are no phase boundaries. Catalysis may take place either in the gas or liquid phase.

2. Heterogeneous: there is a phase boundary separating the catalyst and reactants. The different phase combinations are given in Table 1.

There is, however, one extremely important group of substances that cannot be accommodated within this classification, namely the enzymes, which are neither homogeneous nor heterogeneous catalysts but they are large, complex organic molecules, usually proteins [7].

Table 1: Number of phase combinations in heterogeneous systems [7]

Catalyst	**Reactant**	**Example**
Liquid	Gas	Polymerization of alkenes catalyzed by phosphoric acid
Solid	Liquid	Decomposition of H_2O_2 catalyzed by Au
Solid	Gas	Ammonia synthesis catalyzed by Fe
Solid	Liquid and Gas	Hydrogenation of nitrobenzene to aniline catalyzed by Pd

For catalysis to occur, a chemical interaction between the catalyst and reactant system is required, with no change in the chemical nature of the catalyst except at the surface. The ability of a substance to act as a catalyst depends on its chemical nature and Table 2 gives a summary of the classification of heterogeneous catalysts [7].

Table 2: Classification of heterogeneous catalysts [7]

Class	Functions	Examples
Metals	Hydrogenation, Dehydrogenation, Hydrogenolysis, Oxidation	Fe, Ni, Pd, Pt, Ag
Semi-conducting oxides and Sulphides	Oxidation, Dehydrogenation, Desulphurization, Hydrogenation	NiO, ZnO, MnO_2, Cr_2O_3, $Bi_2O_3 – MoO_3$, WS_2
Insulator oxides	Dehydration	Al_2O_3, SiO_2, MgO
Acids	Polymerization, Isomerization, Cracking, Alkylation	H_3PO_4, H_2SO_4, SiO_2-Al_2O_3, Zeolites

Transition metals are good catalysts for reactions involving hydrogen and hydrocarbons because they readily adsorb these substances on their surface. Base metals are not good for oxidation because they are rapidly oxidized throughout the bulk at the required reaction temperature. Only noble metals are resistant to corrosion and may be used for oxidation reactions. Alumina, silica, and magnesia do not interact with oxygen and therefore they are poor oxidation catalysts, but they readily adsorb water and can be used to catalyze dehydration. The oxides used for hydrogenation must be resistant to reduction by hydrogen at the temperatures at which they are active [7].

1.3 Requirements for a Catalyst

A catalyst must be able to effect the desired reaction at an acceptable rate under practicable conditions and sustain the reaction over prolonged periods. The longer it lasts, the smaller the contribution its initial cost will make to the overall cost of the process. It must also be selective, reflecting its ability to direct conversion of reactants along one specific pathway.

Side reactions must be minimal, especially the ones that lead to poisoning and/or deactivation. Reversible poisoning due to the presence of either impurities in reactants or side reactions and irreversible physical changes, such as fouling, loss of surface area or mechanical failure, are the main causes of catalyst deterioration [9].

For reactions in general, a plot of conversion against temperature is obtained. The conversion depends on the contact time or the gas flow rate, the amount of catalyst used as well as on the loading (type, percentage etc.) of the active component.

At low conversion the rate is limited by the catalytic process known as the kinetic regime, but as the rate increases and becomes faster than the rate of diffusion of reactants to the surface it becomes limited by mass transfer, known as the diffusion regime. Deactivation of a catalyst can be estimated by following conversion as a function of time at a fixed temperature [9].

1.4 History of Catalysis

Catalysis is at the heart of both the chemical and the petrochemical industries, the production of fuel, foodstuffs, pharmaceuticals and other numerous manufactured goods. Industrial catalysis plays a huge role in the creation of wealth and the great achievements reached in the 20^{th} century demonstrates this. It has been applied for thousands of years in processes such as fermentation, production of H_2SO_4 etc. [9].

Its history dates back to the beginning of civilization when humankind began to produce alcohol by fermentation. Catalysis is the means through which many syntheses are achieved. In the present day, it is increasingly applied in the suppression of atmospheric pollution, in the design of environmentally compatible new technologies and in the pursuit of new ways of generating energy and materials. More than 90% of the chemical manufacturing processes in use throughout the world utilize catalysts in one form or another [9].

The period of catalysis that can be characterized by the continuous invention of new catalytic processes, has clearly not yet passed. The point in time when the transition into a new era will take place is at present not easy to predict. What we can say with certainty, however, is that the future of catalysis will be as exciting tomorrow as it was during the early years [10].

1.5 References

1. M.A. Debeila, R.P.K. Wells and J.A. Anderson, *J. Catal*., **239** (2006) 162.
2. W.-S. Lee, B.-Z. Wan, C.-N. Kuo, W.-C. Lee and S. Cheng, *Catal. Comm*., **8** (2007) 1604.
3. C.H. Kim and L.T. Thompson, *J. Catal*., **230** (2005) 66.
4. N.A. Merino, B.P. Barbero, P. Grange and L.E. Cadús, *J. Catal*., **231** (2005) 232.
5. B.P. Barbero, J.A. Gamboa and L.E. Cadùs, *Appl. Catal., B: Environ*, **65** (2006) 21.
6. S. Colonna, S. De Rossi, M. Faticanti, I. Pettiti and P. Porta, *J. Mol. Catal. A*, **180** (2002) 161.
7. C.G. Bond, Heterogeneous Catalysis, Principles and Applications, Oxford University Press, New York, 1987.
8. J.B. Jiggins, *Catal. Today*, **19** (1994) 7.
9. J.M. Thomas and W.J. Thomas, Principles and Practices of Heterogeneous Catalysis, Weinheim, New York, Basel, Cambridge, Tokyo, VCH, 1996.
10. B. Lindström and L.J. Petterson, *CATTECH*, **7** (2003) 130.

CHAPTER 2

2 GOLD IN CATALYSIS

The chemistry of gold and its complexes has been a subject of interest for many years. Colloidal gold has attracted a lot of attention and this chapter summarizes the structure, characteristics, uses and applications of gold, especially in carbon monoxide oxidation reactions.

2.1 Background

Actual mining of gold started around 3500 B.C but this valued commodity was known and treasured long before that. Naturally, gold occurs as alluvial or in lodes or veins and replacement deposits. Gold has a lot of applications like in medicine but most importantly it is used in trade and this has caused a lot of political and economical uncertainties [1].

Before the 1980s gold did not play a major role in catalysis due to the presence of impurities in the solid, but it is now considered to be extremely active for some reactions when deposited on certain supports [2]. Gold is known as one of the most stable metals among the elements that are resistant to oxidation and other harsh environments. This is why the discovery that gold is capable of being a very active catalyst when highly dispersed made a great impact on the scientific community [3].

Gold is found in group eleven in the periodic table, in the same group as silver and copper. It lies between platinum and mercury. Mercury is generally toxic, whilst platinum is a versatile catalytic metal. Gold has been used as a second component in platinum-based alloys, the gold being considered as immiscible with platinum and found to segregates to the platinum surface [3]. Figure 1 compares some properties of gold with respect to its neighbours.

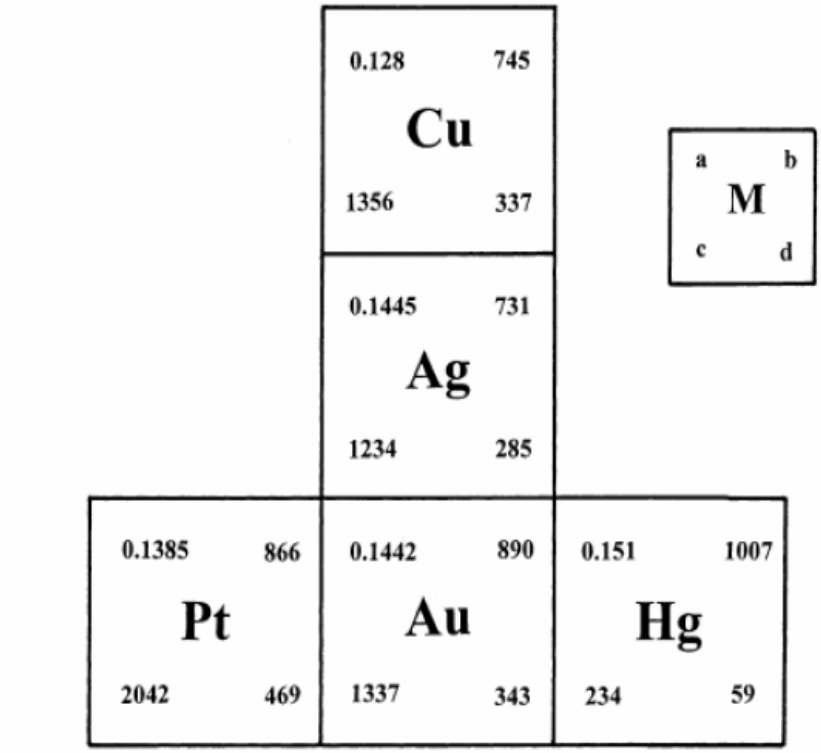


Figure 1: Some physical properties of platinum, mercury and the metals of group II.

a - metal radius (nm);
b - first ionization potential (kJ/mol);
c - melting temperature (K);
d - sublimation enthalpy (kJ/mol) [5]

2.2 Properties, characteristics, uses and chemistry of gold

Gold is a soft, malleable yellow metal. It is highly conductive and has been used for electrical wiring in some high energy applications. It is unique in a number of ways – it is the most electronegative metal (2.54), with an electron affinity greater than that of oxygen [6].

Gold readily forms alloys with other metals [7, 8] giving intermetallic compounds of definite composition with copper, aluminium, tin and titanium [8]. It exhibits all the properties of the metal in terms of lustre, hardness, ductility, malleability, etc. It will not react directly with other electronegative elements such as sulphur or oxygen, as well as with common acids, but is attacked by aqua regia (a three-to-one mixture of HCl and nitric acid). Some of the basic properties of gold are listed in Table 3 [4].

Table 3: Basic properties of gold [4]

Symbol	**Au**
Atom number	79
Electron configuration	$[\,Xe\,]\,4f^{14}\,5d^{10}\,6s^{1}$
Density	196,97 g/mol
Metallic radius	144,20 pm
Melting point	1337 K
Boiling point	3081 K

Gold is stable and inert which results in it being used in electrical circuitry and recent advances in gold nanotechnology signal exciting new developments. It is used for IR reflective coatings on glass for aircraft cockpit/space shuttle windows and architectural glass in office buildings. Gold foil is used for decorative gilding coatings in, for example, books, church furniture, steeples and statues. This element is also found in ceramic tableware and glassware. Table 4 gives a summary of some of the uses of gold [4].

Table 4: Other gold uses [4]

Form of gold	**Some uses**
Gold salts	Have anti-inflammatory properties and are used as pharmaceuticals in treatment of arthritis and similar conditions
Gold-leaf, flake or dust	Used in gourmet foodstuffs i.e. sweets and drinks as a decorative ingredient
Gold alloys	Used in restorative dentistry
Gold toners	Used in photography
Colloidal gold	Used in medicine, biology and materials science

The differences in the chemical behaviour of gold compared to copper and silver, particularly the resistance of gold to oxidation, can be attributed largely to the impact of a relativistic effect as explained by Raphulu [4]. In Table 5, the different properties of gold as compared to other metals are shown.

Table 5: Comparison of the properties of Au with Ag and Cu [4]

Property	**Cu**	**Ag**	**Au**
Atomic number	26	47	79
Electron configuration	$[Ar]3d^{10}4s^{1}$	$[Ar]4d^{10}5s^{1}$	$[Xe]\ 4f^{14}5d^{10}6s^{11}$
Structure	FCC	FCC	FCC
Lattice constant (nm)	0.361	0.409	0.408
Metallic radius (nm)	0.128	0.1445	0.1442
Density (g/cm^3)	8.95	10.49	19.32
Melting temperature (K)	1356	1234	1337
Boiling temperature (K)	337	285	368
Electron affinity (eV)	1.228	1.202	2.039
Heat of atomization (kJ/mol)	338	285	368
Ionization potential (kJ/mol) 1^{st}	746	730	890
Ionization potential (kJ/mol) 2^{nd}	1958	2073	1980

There are clear differences between gold, copper and silver, for example, the usual trends that are expected within a group in the periodic table are not uniformly found in group eleven metals. For instance, the atomic radius measurements show that the Au atom is slightly smaller than the Ag atom and the same is true for the Au(I) and Ag(I) ions. This is attributed to the lanthanide contraction. The consequences of the relativistic effect have an impact on metallic gold being more resistant to oxidation than silver [4].

2.3 Gold as a Catalyst

Bulk gold has long been known to be chemically inert, but small gold particles appear to be extremely active catalytically. An example of the known catalytic application of gold is in carbon monoxide oxidation at low temperatures [9]. In the present study, gold supported on perovskite catalysts for low temperature carbon monoxide oxidation has been studied, which to our knowledge, has not been explored to date.

Since the 1980s, when gold was considered inert, there have been many interesting findings regarding the activity of gold nanoparticles as a catalyst. The chemistry of these nanoparticles has been widely studied in an attempt to understand the different reactions that have been reported to be catalysed by these nanoparticles.

The first example of a reaction for which a gold catalyst was the catalyst of choice over many others was demonstrated by Hutchings on the hydrochlorination of acetylene to vinyl chloride, which exhibited a very high activity. The study demonstrated clearly that any metal cation with a higher electrode potential than that of Hg^{2+} should give enhanced catalytic activity. On this basis gold cations should be the most active. Subsequent research confirmed this prediction and gold catalysts were found to be about three times more active than the commercial mercuric chloride catalyst [10].

Other demonstrations of gold activity were described by Haruta, at the Osaka National Research Institute in Japan, who reported gold to be extremely active for some reactions if deposited on various supports [9]. Haruta was the first person to show that gold could be effective for CO oxidation at ambient temperature. When gold was co-precipitated with certain metal oxide supports, Haruta found that the resulting catalysts were very active for carbon monoxide oxidation. After testing a range of metal oxide supports, he observed that the best results were obtained with α-Fe_2O_3 and a gold loading of 5%.

Nowadays gold catalysis is receiving increasing attention from a number of research groups around the world, and the subject has been extensively reviewed by Bond and Thompson [11, 12].

The relatively new field of gold catalysis has diverse and promising applications, but CO oxidation is the reaction that has received the most attention. It represents one of the key processes in the fractionation of molecules *via* selective oxidation or the removal of pollutants *via* total oxidation. Oxidation is used in many processes and therefore influences everyday life in a way similar to the impact of catalysis in general. The designing of oxidation catalysts is therefore one area in research that has attracted a lot of interest in recent times [13].

There are countless possible applications for the use of gold in CO oxidation reactions [14, 15, 16, 17], which include:

- car exhaust systems for pollution control
- fuel cells (CO purification in $H_2 + O_2$ streams)
- gas sensing and
- chemical processing (CO oxidation in reforming gas)

However, any practical applications of a catalyst will require a reliable method of preparation, long-term stability, good response to operating conditions, and more information on the kinetics and mechanism of the reaction.

The explanation of the causes and mechanism of the outstanding low temperature activity of gold catalysts for CO oxidation is expected to receive more attention, not only because of practical applications of this reaction but also because it will provide insight into the more general field of heterogeneous catalysis [18].

The following reactions have also been shown to be effectively catalysed by supported gold catalysts:

- Catalytic combustion of hydrocarbons
- Water gas shift reaction
- Selective oxidation e.g. epoxidation of olefins
- Selective hydrogenation, e.g. of alkynes and dienes to mono olefins
- Hydrochlorination
- Reduction of NO_x with propene, carbon monoxide or hydrogen
- Hydrogen and oxygen reaction to give hydrogen peroxide

The catalytic activity of supported gold catalysts has been shown to depend on a number of factors that can be fine-tuned either before catalyst preparation, (e.g. choice of support and gold precursor) or during the preparation process, (e.g. variables such as temperature, pH, and method of preparation). Even after preparation, conditions of pre-treatment prior to use in reactions and storage conditions are important. These factors may depend on each other or may vary from one reaction to the next or from one catalyst to another. There is, thus, considerable confusion on these issues and there are discrepancies in the literature on the effects of these factors.

2.4 Methods of preparing gold catalysts

The method of preparation is one of the factors known to have an effect on catalytic activity. There are many variables to be considered when preparing a catalyst, and any small variation in these can lead to differences in activity and stability. For example, in the deposition–precipitation method, the surface properties of the support will strongly affect the final dispersion of the gold particles [19, 20].

Small metal particles are unstable with respect to bulk gold, so the support must have a suitable surface area which keeps the gold particles apart. A strong interaction between the gold particles and the surface of the support is thus required to stabilize them and to avoid sintering, especially if the catalyst is calcined. Different researchers have thus spent much time studying different methods of preparation and the effect they play on catalysis by gold nanoparticles. The following methods of preparation have been reported for gold catalysts [17]:

2.4.1 Deposition–precipitation method

Among the available methods for preparing highly dispersed gold nanoparticles, the deposition-precipitation method is one of the most successful, where the gold precursor, typically chloroauric acid ($HAuCl_4$) is brought out of solution in the presence of a suspension of the support by raising the pH in order to precipitate $Au(OH)_3$. The optimal experimental conditions for obtaining gold nanoparticles by the deposition-precipitation method are dependent on the different supports used.

The deposition-precipitation and co-precipitation method provide the desired intimacy of contact between the metal and the support. However, deposition-precipitation has the advantage over co-precipitation because all of the active component remains on the surface of the support and is not buried within it. Also, it gives a narrower particle size distribution.

2.4.2 Impregnation method

For impregnation, the gold precursor, usually $HAuCl_4$ or $AuCl_3$ is dissolved in water in quantities which correspond to the desired metal loading, followed by wet impregnation of the support material (e.g. SiO_2, TiO_2, ZrO_2) present in powder form or as extrudates. After drying, calcination and a subsequent reduction in hydrogen at elevated temperatures (473–773 K) the final supported gold catalyst is obtained.

2.4.3 Precipitation method

An aqueous solution of the gold precursor is adjusted to a fixed value of pH ranging from 6-10, and the preformed support material is added (deposition-precipitation, DP). Alternatively the support can be precipitated simultaneously with the gold solution (co-precipitation, CP). After further stirring and aging of the solution, the precipitate is dried, washed several times in an appropriate solvent and then filtered, calcined and reduced in a similar manner as for impregnation.

2.4.4 Ion-exchange method

The ion-exchange method involves cation exchange by which protons or other cations on the surface or within the structure of the support are replaced by cations of the active metal, e.g. noble elements of group 8-10. This gives atomically dispersed species. After calcination the metal ions are carefully reduced with hydrogen to give very small metal particles. The procedure is especially effective with zeolites.

2.4.5 Vapour-phase deposition and grafting method

These two methods are similar and differ only in whether a solvent is used or not. In the vapour-phase method, a stream of a volatile compound of gold is transported to a high surface area support by an inert gas, and it reacts with the surface of the support to form a precursor of the active species. This method is suitable for acidic supports e.g. alumina-silica and non-metal oxide supports such as activated carbon for which deposition-precipitation would be inoperative. In the grafting method, a gold complex in solution reacts with the surface of a support to form some species capable of being converted to a catalytically active form. The solution can be in the gas phase (gas phase grafting) or liquid phase (liquid phase grafting).

2.4.6 Co-sputtering method

In an oxygen containing atmosphere, gold and the metal oxide are simultaneously sputter-deposited onto a substrate, leading to the formation of a thin film, which is then annealed in air.

2.4.7 Colloidal mixing method

A colloidal solution of gold is diluted with isopropyl ether, followed by the addition of the powder of metal oxide support to make an organic suspension. After stirring for an hour, the organic solvent is evaporated in a vacuum at 373 K for 4 h, and the dried Au-metal oxide mixture then calcined in air at temperatures between 473 and 873 K.

2.4.8 Other methods

Other less widely used methods include, a novel approach for the synthesis of supported gold catalysts referred to as the single step borohydride (SSBH) method that was recently reported by Mallick and Scurrell [21]. A pulsed laser deposition (PLD) method, with appropriate control of the amount of deposited material has been used by Guczi *et al*. to produce model $Au/FeO_x/SiO_2/Si$ (100) catalysts for CO oxidation [22].

2.5 Characterisation of Gold Catalysts

In an attempt to understand the chemistry of gold nanoparticles and, most importantly, to gain an insight into heterogeneous catalysis in general, catalyst characterization also plays a very important role. Information such as the interaction of the catalyst with the product and reactant, the required particle size for the catalyst to be active, and the oxidation state of the active catalyst is essential for a knowledge of catalyst morphology and a whole branch of research has been dedicated to catalyst characterization. Gold catalysts have been characterised using the following methods:

2.5.1 Transmission Electron Microscopy (TEM)

TEM has traditionally been used to observe the size, shape and surface structure of the active sites that define the catalytic performance of Au [23, 24, 25, 26, 27, 28].

2.5.2 Nitrogen physiosorption (BET surface area)

In general, for gas reactions catalyzed by solid materials, the formation of the product depends, amongst other factors, on the available surface area – the greater the surface area accessible to reactants, the larger is the amount of reactant converted to product per unit mass of catalyst. This method of determining surface area was developed by Brunauer, Emmet and Teller (BET), and the surface area derived is usually called the BET surface area, denoted as S_{BET} and is expressed in m^2/g [29, 30, 31].

2.5.3 X-Ray Diffraction (XRD)

Firstly, XRD gives information as to whether the catalyst or a component of it is crystalline, non-crystalline or quasi-crystalline. Secondly, it can be used to estimate the size of the gold crystallites present in the catalyst by using the Scherrer equation. Thirdly, it gives an insight into the atomic constituents of the unit cell from the d-spacing and unit cell dimensions, and lastly, in favourable circumstances, from in-situ experiments, it can predict what influence the reactant gas exerts upon the internal structure as well as the crystalline order of the exterior surface of the catalyst [32].

2.5.4 Inductively Coupled Plasma (ICP) Elemental Analysis

This technique has been widely used to determine the gold content of the supported gold catalysts, since in most cases the actual gold loading is always lower than the intended gold loading. Either atomic emission or absorption spectroscopy is applied [29, 31, 33].

2.5.5 Photoelectron spectroscopy (X-Ray and UV-induced)

X-Ray photoelectron spectroscopy (XPS) and UV-induced photoelectron spectroscopy (UPS) can give information about the local chemical environment and bonding of the metals [16, 22, 34].

2.5.6 Infrared (IR) Spectroscopy

Infrared spectra give information on the physiochemical properties of surface complexes, the forms of adsorption on the substrate and molecular changes occurring during adsorption. Most of this information is important for elucidating mechanisms for adsorption and catalysis [33].

2.5.7 Extended X-ray absorption fine structure (EXAFS)

EXAFS provides detailed information about the local atomic structure and is analyzed by curve fitting. EXAFS has been used to study supported gold catalysts and to evaluate quantitatively the ratio between oxidized and reduced states of gold on the support surface [32, 35].

2.5.8 Mössbauer Spectroscopy

This method is used primarily to study the electron states of some metals like gold and iron in materials. It is an element-selective technique and sensitive to the local surroundings of the atoms making it possible to resolve the different metal sites within the catalyst particles and thereby differentiating between metal atoms at the surface and atoms in the inner-core of the particles [31].

2.5.9 Other methods

Other methods that have been used, to a lesser extent, to characterize supported gold catalysts include:

- Diffuse reflectance ultraviolet/visible (DR-UV/vis) spectroscopy to examine the electronic state of Au in various catalysts [26].

- Temperature programmed techniques such as temperature programmed desorption (TPD) to monitor the adsorption of reactant gases on different Au species [35], temperature programmed reduction (TPR) and temperature programmed oxidation (TPO) to quantatively determine amounts of different gold species present in an operating catalyst, to determine suitable conditions for the removal of carbonaceous deposit and to determine the temperature at which the support changes chemical state [29].

- Atomic absorption spectroscopy (AAS) for accurate determination of the gold loading on the support [26, 27].

2.6 Summary

To understand the chemistry of gold nanoparticles and their role in the catalysis of different reactions, it is important to fine-tune all these variables to develop a catalyst that is active and stable. Characterization of the catalysts is essential and with constant advances in technology, it is becoming easier to obtain a better understanding of gold chemistry.

For example, the recent results from Hutchings and co-workers [36] on the use of aberration-corrected STEM to identify the active Au nanoclusters available on iron oxide support for CO oxidation. We can therefore agree with Lindström ***et al.*** [37] with certainty that the future of catalysis will be as exciting tomorrow as it was during the early years.

2.5 References

1. Website: www.Madehow.com/vol-1/Gold.html, Accessed on 30/01/2006.
2. M. Haruta, *CATTECH*, **6** (2002) 102.
3. D.I. Hagen and G.A. Somarjai, *J. Catal*., **41** (1971) 466.
4. M.C. Raphulu, PhD Thesis, "Catalytic oxidation of carbon monoxide and methane with gold based catalysts", University of the Witwatersrand, (2005).
5. G.C. Bond, *Catal. Today*, **72** (2005) 5.
6. C. Mohr, H. Hofmeister, M. Lucas and P. Claus, *Chem. Eng. Tech.*, **23** (2000) 324.
7. V. Ponec and G.C. Bond Catalysis by Metals & Alloys, Elservier, Amsterdam, 1996.
8. D. Guillemot, V.Y. Borovkov, V.B. Kazansky, M. Polisset-Thfoin, and J. Fraisard, *J. Chem. Soc. Faraday Trans*., **93** (1997) 3587.
9. M. Haruta, N. Yamada, T. Kobayashi, S. Iijima, *J. Catal*., **115** (1989) 301.
10. G.J. Hutchings, *Catalysis*, **96** (1985) 282.
11. D.T Thompson and G.C. Bond, *Catal. Rev.-Sci. Eng*., **41** (1999) 319.
12. G.C. Bond and D.T. Thompson, *Gold Bull.*, **33** (2000) 41.
13. G.J. Hutchings and M.S. Scurrell, *CATTECH*, (2003), 90.
14. M.N. Desai, J.B. Butt and J.S. Dranoff, *J. Catal*., **79** (1983) 95
15. M.J. Kahlich, H.A. Gasteiger and R.J. Behm, *J. Catal*., **182** (1999) 430
16. M. Haruta, T. Kobayashi, S. Tsubota and Y. Ankara, *Chem. Express*, **5** (1998)
17. J.A. Moma, PHD Thesis "Carbon Monoxide Oxidation over Modified Titanium Dioxide Supported Gold catalysts", University of the Witwatersrand, (2007).
18. Y.M. Kang and B.Z. Wan, *Catal. Today*, **35** (1997) 379
19. C.G. Bond, *Catal. Rev. Sci. Eng*., **41** (1999) 321.
20. D.T. Thomson, *Gold Bull.*, **31** (1999) 111.

21. K. Mallick and M.S. Scurrell, *Appl. Catal. A: Gen.,* **253** (2003) 527.
22. L. Guczi, K. Frey, A. Beck, G. Petŏ, C. S. Daróczi, N. Kruse and S. Chenakin, *Appl. Catal. A: Gen*., **291** (2005) 116
23. A. Pantelouris, G. Kuper, J. Hormes, C. Feldmann and M. Jansen, *J. Am. Chem. Soc*., **117** (1995) 11, 749.
24. J. Guzman and B.C. Gates, *J. Phys. Chem, B*, **107** (2003) 2242.
25. A. Goossens, M.W.J. Cranjé, A.M. van der Kraan, A. Zwijnenburg, M Makkee, J.A. Moulijn and L.J de Jongh, *Catal. Today*, **72**, (2002,) 95.
26. F.E. Wagner, S. Galvagno, C. Milone, A.M. Visco, L. Stievano and S. Calogero, *J. Chem. Soc. Faraday Trans.*, **93** (1997) 3403.
27. J.L. Margitfalvi, A. Fási, M. Hegedűs, F. Lónyi, S. Gőbölös and N. Bogdanchikova, *Catal. Today*, **72** (2002) 157.
28. J.M.C. Soares and M. Bowker, *Appl. Catal. A: Gen.,* **291** (2005) 136.
29. J.L. Margitfalvi, Á. Szegedi, M. Hegedűs and I. Sajó, *Appl. Catal. A: Gen.,* **272** (2004) 87.
30. M. Khoudiakov, M.C. Gupta and S. Deevi, *Appl. Catal. A, Gen*., **291** (2005) 151.
31. M. Valden, S. Pak, X. Lai and D. W. Goodman, *Catal. Lett*., **56** (1998) 7.
32. B. Lindström and L.J. Petterson, *CATTECH*, **7** (2003) 130.
33. S. Minicò, S. Scirè, C. Crisafulli, A.M. Visco and S. Galvagno, *Catal. Lett*., **47** (1997) 273.
34. B. Qiao and Y. Deng, *Chem. Commun*., (2003) 2192.
35. G.K. Bethke and H.H. Kung, *Appl. Catal. A, Gen*., **194** (2000) 43.
36. A.A. Herzing, C.J. Kiely, A.F. Carley, P. Landon and G.J. Hutchings, *Science*, **321** (2008) 1331.
37. B. Lindström and L.J. Petterson, *CATTECH*, **7** (2003) 130.

CHAPTER 3

3 PEROVSKITES

Materials with the perovskite structure, or topologically closely related structures, have been of central interest to many solid-state scientists over the past decades. This chapter summarizes the structure, characteristics, properties and applications of perovskites.

3.1 Introduction

The perovskite, $CaTiO_3$ is a rare mineral that was discovered in the Ural Mountains of Russia in 1839 and named after the Russian mineralogist, L. A. Perovski. Many oxides adopt the perovskite structure with the chemical formula ABO_3 and possibly have the same crystal structure. This mineral can be found in metamorphic rocks that are associated with mafic intrusives, as well as in some silica-undersaturated igneous rocks (e.g. malilite) and in calcium-aluminium-rich inclusions found in some chrondritic meteorites [1].

The A-sites may be occupied by rare-earth, alkaline-earth, alkali or other large ions and the B sites are usually filled with transition-metal cations. It is well documented that the activity of these oxides is controlled by the nature of the B-site.

The high stability of the perovskite structure allows the partial substitution of either the A or B sites or both and the consequent creation of structural defects such as anionic or cationic vacancies and/or a change in the oxidation state of the transition metal cation to maintain the electroneutrality of the compound [2].

Figure 2 shows the general crystal structure of a perovskite, which is a primitive cube, with the A-cation in the middle of the cube, the B-cation in the corner and the anion, commonly oxygen, in the centre of the faces edges. The structure is stabilized by the 6-fold coordination of the B-cation (octahedron) and 12-fold coordination of the A cation [1].

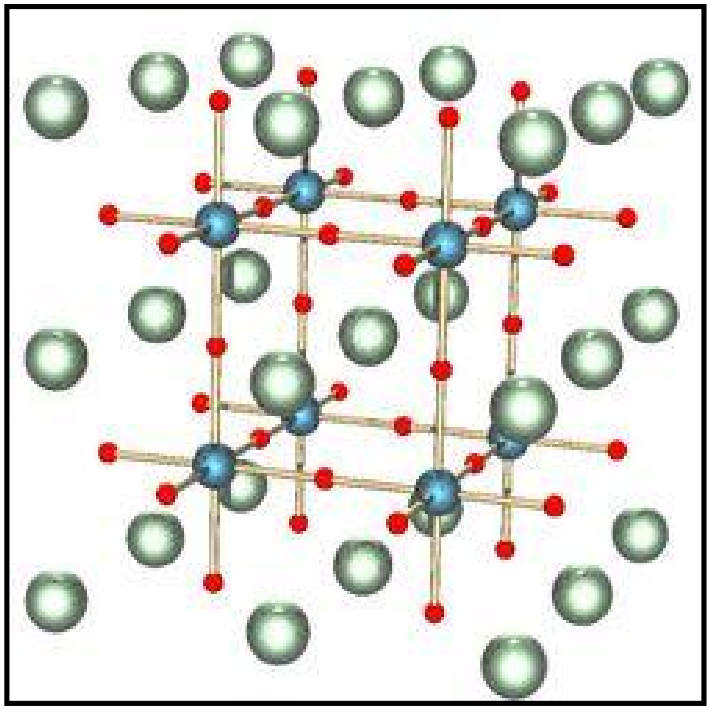


Figure 2: The general perovskite structure [1].

- Red spheres represent oxygen,
- Blue spheres represent the small metal cations (B) and
- Green spheres represent the larger metal cations (A) [1]

The packing of the ions can be thought to form a cubic close packed array, where the B ions occupy a quarter of the octahedral holes. When the ratio of the ionic radii differs too much, distortion occurs; with tilting being the most common outcome. With perovskite tilt the BO_6 octahedron twists along one or more independent axes to accommodate the ratio-difference [1].

3.2 Properties, Uses and Characteristics of Perovskites

Oxides with the perovskite structure show characteristic features in their physical behavior; the most outstanding feature is that due to its topology (i.e. the principal arrangement of atoms). Perovskite is thermodynamically extremely stable, whereas its actual crystal structure (i.e. the actual position of the atoms) appears to be very unstable. Virtually all perovskites have a lowered symmetry via a structural phase transition. The colour varies from black, brown, gray and orange to yellow. They generally have low surface areas [3].

Perovskites have considerable technological importance due to their rich crystal chemistry and structure-property relationships. Their applications as outlined by Googneough [4] include use as:

- Multilayer capacitors
- Oxidation catalysis
- Piezoelectric transducers
- Thick film resistors
- Electronic sensors
- Batteries
- Ceramic electrodes
- High temperature super-conductors etc.

The properties of perovskites in powder form are greatly affected by their characteristics, such as particle size, morphology, purity and chemical composition. Using chemical methods like co-precipitation, sol-gel, hydrothermal and colloid emulsion techniques, it is possible to efficiently control the morphology and chemical composition of the prepared powder. Among these wet chemical techniques, sol-gel methods using alkoxides, hydrothermal and colloid emulsions are time-consuming and involve highly unstable alkoxides and reaction conditions that are difficult to maintain.

In our study we opted to use the citrate method [5] which avoids complex steps such as the refluxing of alkoxides and is quicker to use. It involves the complexation of metal ions by poly-functional carboxyl acids such as citric acid or tartaric acid having one hydroxyl group. On heating, the solvent (water) evaporates resulting in increased viscosity. On complete removal of water, the mixture is a polymeric gel and its constituents mixed at the atomic level. This resin on heating at higher temperature produces the respective oxides. The citrate method also offers a number of advantages such as good control of chemical stoichiometry and low processing conditions for the preparation of fine powders of many complex oxides [5].

3.3 Oxidation Catalysis using Perovskites

Catalytic oxidation using perovskites was first reported in the early 1950's but the most interesting findings were from investigations conducted in the 1970's. Meadowcroft [6] reported a perovskite-type catalyst, which showed high activity for the electrochemical reduction of oxygen.

Subsequently, many studies were undertaken to explain the chemistry of perovskites as catalysts in electrocatalysis, auto-exhaust treatment and catalytic combustion. A large number of studies have therefore been published concerning the oxidation catalysis by perovskite-type oxides. A detailed investigation by Yamazoe and Teraoka [7] gives an overview of the different types of reactions catalyzed by perovskite-type catalysts. Table 6 is a summary of some of the work that has been reported on perovskites as catalysts for different reactions.

Table 6: Perovskite-type oxides as oxidation catalysts [6]

Reaction	**Catalyst**
CO to CO_2	$LaBO_3$ (B = 3d transition metals),
CH_4 to CO_2, H_2O	$LaBO_3$ (B = 3d transition metals)
C_2H_4 to CO_2, H_2O	$LaBO_3$ (B = Co, Mn)
C_3H_6 to CO_2, H_2O	$LaBO_3$ (B = Cr, Mn, Fe, Co, Ni)
C_3H_8 to CO_2, H_2O	$LaBO_3$ (B = Co, Mn, Fe)
CH_4 to C_2H_6, C_2H_4	ABO_3 (A = Ca, Sr, Ba, B = Ti, Zr, Ce)
$C_6H_5CH_3$ to C_6H_5CHO	$LaCoO_3$

Perovskite-type oxides are cheap, tolerant to high temperatures and have been found to be active in different reactions including those catalyzed by noble metals such as Pt and Pd. They are therefore potential substitutes for the Pt-based catalysts.

Buciuman and his colleagues [8] studied the substitution effects on the reducibility of $La_{0.8}A_{0.2}MnO_{3+\delta}$ perovskites, where A = Sr, Ba, K, Cs and $\delta = 0.16$ for $LaMnO_3$, 0.07 for Sr, 0.06 for Ba, 0.07 for K and 0.03 for Cs. They concluded that alkali and alkali-earth substituted lanthanum manganites show an enhanced reducibility at low temperatures as compared to the non-substituted perovskites. These perovskites have a great capability of releasing important amounts of lattice oxygen at low temperature, which has been reported to play a role in the catalyst activity.

Merino *et al*. [2] carried out a study on $La_{1-x}Ca_xCoO_3$ (x = 0, 0.2, 0.4, 0.5) and showed that the perovskite composition may be changed by partial replacement of A and/or B cations with other metals. Such substitutions produced modifications of the perovskite's catalytic behavior. The substitution effects on the catalytic activity depended on both the reagent molecule involved and the oxidation mechanism. A perovskite catalyst with La at the A-site and Co on the B-site provided excellent catalytic activity for oxidation. Such activity was further improved by replacement of La with Sr or Ce. Substitution of La by Ca increased the surface area but decreased the crystallinity of the catalysts.

Barbero *et al*. [9] synthesized and characterized $La_{1-x}Ca_xFeO_3$ perovskite-type oxide catalysts for the total oxidation of volatile organic compounds. XRD diffraction lines broadened and decreased in intensity as the calcium content increased. The FT-IR band around 877 cm^{-1} which was due to the presence Fe^{4+} ions as a result of Fe being oxidized to compensate for the electoneutrality also broadened and decreased. From their results they concluded that as the calcium content increased a change in the crystalline structure of the perovskite led to an increase in the oxidation state of iron from Fe^{3+} to Fe^{4+} to maintain the electroneutrality.

Ciambelli *et al*. [10] showed that oxygen vacancies are also formed to conserve the catalyst electroneutrality. In correlating their characterization and activity results, they concluded that the active sites for these catalysts were associated with Fe^{4+} ions.

The methods used for the preparation and the distribution or dispersion of the metal have been reported to affect either the activity or the stability of the catalysts. Takehira *et al.* [11] performed work on Ni catalysts supported on perovskite-type oxides prepared by a solid phase crystallization method for the CO_2 reforming of CH_4 into synthesis gas. Ni/$Ca_{0.8}$ $Sr_{0.2}TiO_3$ and Ni/$BaTiO_3$ catalysts showed high activity and stability. The superior activity was due to the highly dispersed and stable Ni metal particles on the perovskite. Enhanced stability was partly due to the mobile oxygen, as well as the presence of alkaline earth metals in the perovskite support. The study showed that there is an easy migration of oxygen from the support to the surface of the Ni particles.

Nishihata *et al.* [12] studied $Fe_{0.57}Co_{0.38}Pd_{0.05}O_3$ catalysts using X-ray diffraction and absorption for analysis. The $LaFe_{0.57}Co_{0.38}Pd_{0.05}O_3$ retained its high metal dispersion owing to structural responses to the fluctuations in composition. When the catalyst was cycled between oxidative and reductive atmospheres, the Pd moved reversibly into and out of the perovskite lattice. The movement appeared to suppress the growth of metallic Pd particles and retained the high catalytic activity during long-term usage and ageing. The comparison between Pd-perovskite and Pd-alumina showed that the Pd-perovskite retained its high activity during ageing while the Pd-alumina deteriorated by 10%. Pd-alumina particles reached a size of up to 120 nm whereas Pd-perovskite reached sizes of 1-3 nm. This suppression of metallic growth directly affected the capability of the Pd-perovskite catalyst to maintain high activity. XRD analysis showed that the perovskite structure is predominant throughout the oxidation, reduction and re-oxidation cycle. It also showed that the Pd occupied the B-site and was in its metallic state in the reduced sample.

It is not easy to maintain the high surface area and avoid sintering when using most of the various methods for perovskite synthesis. González *et al.* [13] synthesized high surface area perovskite catalysts by non-conventional routes.

They synthesized the perovskite $NdCoO_3$ under calcination conditions: from heteronuclear organic complexes or amorphous precursors obtained by freeze-drying of nitrate solutions which resulted in the synthesis of relatively high surface area materials.

Depending on the method used, different features were obtained:

- various degrees of homogeneity in the bulk distribution of the component cations,
- oxygen non-stoichiometry, as well as
- a range of surface Co/Nd ratios.

It was found that in this way, the synthesis route determines not only the surface area but also the intrinsic activity per surface area for the total oxidation of hydrocarbons.

Zhang-Steenwinkel *et al*. [14] determined the surface properties and catalytic performance in CO oxidation reactions of cerium substituted lanthanum-manganese oxides. These catalysts demonstrated a high activity for CO oxidation and they were stable at high temperatures in an oxidation environment, where their specific surface area and the oxidation activity were barely affected. In contrast, in a reducing atmosphere, the perovskites readily decomposed to the oxides of the individual metals and the activity was lost. Substitution of La for Ce resulted in an enhanced activity for CO oxidation.

XRD and TEM data led to the conclusions that Ce cannot be accommodated in the perovskite beyond a degree of substitution of $x = 0.1 – 0.2$; the excess Ce formed a separate catalytically inert CeO_2 phase. For this reason the catalytic activity decreased beyond $x = 0.2$. XPS data showed that the substitution of La by Ce is accompanied by an increasing concentration of cation/anion vacancies in the perovskite, which in turn led to a shift in the Mn^{4+}/Mn^{3+} ratio.

It was suggested that the number of cation/anion vacancies is directly related to the catalytic activity for CO oxidation by facilitating the CO adsorption, explaining why up to x = 0.2 the activity of La-Mn increased.

Kuhn and Ozkan [15] investigated the surface properties of Fe-based perovskite-type oxides with the formula $La_{0.6}Sr_{0.4}Co_yFe_{1-y}O_{3-\delta}$. Methanol was found to be the appropriate probe for measuring surface site type and density in mixed perovskite-type oxides. They found a non-linear trend with regard to Co content to agree with the strength of the basic sites, reducibility, oxygen storage capacity and B-site composition at the surface. The trends were linked to a possible electronic structure transition and they concluded that the different nature of the sites was likely to lead to the different activities for the different reactions.

From the literature review above it is evident that perovskites have been studied widely due to their unique properties which have led to a number of applications. There has not been much work carried out on perovskites as supports for gold nanoparticles except for the recent work by Russo *et al.* [16] who investigated perovskite-type oxides as supports for gold nanoparticles in the regeneration of diesel particulate filters. Their study showed that the activity of the catalysts towards CO oxidation significantly increased with the presence of gold enhancing the rate of activity. They also showed that the activity does not result exclusively from the Au, but the support itself may be involved in the reaction mechanism. $Au/LaNiO_3$ was the best performing catalyst with a T_{50} = 156°C and T_{100} = 196°C.

3.5 Motivation of Study

Pure perovskites have been investigated as catalysts for high temperature CO oxidation and were found to be active. However, they have never, to our knowledge, been used as supports for gold nanoparticles for low temperature CO oxidation.

Perovskites are very stable and allow partial substitution of either A and B-site cations or both, by other metals with different oxidation states. As a consequence, structural defects such as anionic or cationic vacancies are created. These vacancies were reported to improve the catalytic activity and stability [9, 10]. A lot of interesting results have been reported using pure $LaFeO_3$ as a catalyst for different reactions, for example, in propane oxidation, methane combustion and high temperature CO oxidation. Not much work has been done on low temperature CO oxidation using $LaFeO_3$. We have thus investigated this perovskite as a support for a CO oxidation catalyst and most importantly the effect of gold loading on the activity. Partial substitution of the A-site by calcium in $LaMnO_3$ and $LaFeO_3$ was found to result in oxygen vacancies being formed and improved activity; thus we also investigated the effect of calcium loading on $LaFeO_3$ for low temperature CO oxidation.

3.5 Aims and Objectives

In this study we were interested in supporting gold nanoparticle on perovskites i.e. $LaFeO_3$ and determining the activity of the catalyst in CO oxidation at low temperatures. A series of perovskites of the type ABO_3 were therefore prepared using the citrate method following the procedure used by Navale *et al.* [5]. Gold nanoparticles were then deposited on the perovskites using the single step borohydride method [17] and activity towards CO oxidation determined. The catalysts were characterized using different techniques such as XRD, XRF, Raman, BET, XPS and ICP.

In a summary, we aimed to

- Prepare a series of perovskites using the citrate method;
- Observe the effect of calcination on perovskite formation, overall activity and stability;
- Determine the effect of Au on the overall activity and stability of the perovskite;
- Determine the effect of catalyst modification i.e. Ca doping on activity and stability;
- Characterise the catalysts using XRD, TEM, XPS, XRF, BET surface area, and Raman spectroscopy techniques.

3.6 References

1. http:/en. Wikipedia. Org/wiki/" Perovskite structure" Accessed 01/03/2007.
2. N.A. Merino, B.P. Barbero, P. Grange and L.E. Cadús, *J. Catal*., **231** (2005) 232.
3. E. Salje, *Phil. Trans. R. Soc. Lond. A*, **328** (1989) 409.
4. J.B. Googneough, *Rep. Prog. Phys*., **67** (2004) 1915.
5. S. Navale, V. Samuel and V. Ravi, *Bull. Mater. Sci*., **28** (2005) 391.
6. D. B. Meadocroft, *Nature* **226** (1970) 847.
7. N. Yamazoe and Y. Teraoka, *Catal. Today*, **8** (1990) 175.
8. F.C. Buciuman, F. Patcas and J. Zsako, *J. Therm. Anal. Calorim.*, **61** (2000) 819.
9. B.P. Barbero, J.A. Gamboa and L.E. Cadùs, *Appl. Catal. B: Environ.*, **65** (2006) 21.
10. P. Ciambelli, S. Cimino, S. de Rossi, L. Lisi, G. Minelli, P. Porta and G. Russo, *Appl. Catal. B: Environ*., **29** (2001) 239.
11. K. Takehira, T. Hayakawa, S. Suzuki, J. Nakamura, T. Uchijima, S. Hamakawa, K. Suzuki and T. Shishido, *Appl. Catal. A, Gen*., **183** (1999) 273.
12. Y. Nishihata, J. Mizuki, T. Akao, H. Tanaka, M. Uenishi, M. Kimura, T. Okamoto and N. Hamada, *Nature*, **418** (2002) 164.
13. A. González, E.M. Tamayo, A.B. Porter and V.C. Corberán, *Catal. Today*, **33** (1997) 361.
14. Y. Zhang-Steenwinkel, J. Beckers and A. Bliek, *Appl. Catal. A: Gen*., **235** (2002) 79.
15. J.N. Kuhn and U.S. Ozkan, *J. Catal*., **253** (2008) 200.
16. N. Russo, D. Fino, G. Saracco and V. Specchia, *Catal. Today*, **137** (2008) 306.
17. K. Mallick, M.S. Scurrell, *Appl. Catal. A: Gen*., **253** (2003) 527.

CHAPTER 4

4 EXPERIMENTAL METHODS

This Chapter describes how different supports and catalysts were prepared. It also describes the reagents, equipment and most importantly characterization techniques that were used in the study. The different techniques used to characterize the surface structure of the catalyst generate different information on the catalysts.

4.1 Reagents

$HAuCl_4.3H_2O$ (Aldrich, 99.99%) was used as the precursor for the Au nanoparticles. Sodium borohydride [$NaBH_4$] (Fluka Chemie) was used to reduce the Au^{3+} in the sample. Ammonium hydroxide [NH_4OH] (SAARCHEM) was diluted to 12.5% using distilled water, and used to maintain the pH around 8 – 8.5 during the preparation of the Au catalyst. The intended gold loading was 1.0-wt% with respect to the support. TiO_2 (P25, Degussa) containing 80% of anatase and 20% of rutile phases and calcium nitrate [$Ca(NO_3)_{2.}3H_2O$] (SAARCHEM, 99%) were used for the preparation of $CaTiO_3$. Lanthanum nitrate [$La(NO_3)_{3.}6H_2O$] (Merck, 99%), iron nitrate [$Fe(NO_3)_3.3H_2O$] (SAARCHEM, 99%), citric acid (Sigma-Aldrich, 99%) and calcium nitrate [$Ca(NO_3)_{2.}3H_2O$] (SAARCHEM, 99%) were used for the preparation of $La_{1-x}Ca_xFeO_{3.}$

All the chemicals were used as received without any further analysis or purification. The following gas mixtures obtained from AFROX were used for the CO oxidation reactions: 10% O_2 balanced in helium and 5% CO balanced in helium.

4.2 Preparation of Supports

4.2.1 Preparation of $CaTiO_3$

$CaTiO_3$ was prepared by a method of hydrothermal synthesis [1]. $TiO_2.xH_2O$ was used as a source of titania and commercial $Ca(NO_3)_2.4H_2O$ used as a source of calcium. TiO_2 (30 g) and 89 g of $Ca(NO_3)_2.4H_2O$ were charged into a stainless steel Teflon-lined autoclave along with 200 ml of deionised water. The pH was adjusted to 13 using KOH. The reaction time was 12 h at a stirring rate of 2 rpm and a temperature of 160 ºC. The stirring was stopped after 12 h and the solution was allowed to age for 48 h. The solution was washed with deionised water until the conductivity of the water was 4.3 ×10 µS. The product was dried at 110ºC for 4 h. Samples from the batch were then calcined at 400°C, 600°C or 800°C overnight.

4.2.2 Preparation of $La_{1-x}Ca_xFeO_3$

$La_{1-x}Ca_xFeO_3$ (where x = 0, 4%, 10%, 16% and 20% molar percentage) was prepared by the citrate method [2]. Iron nitrate, lanthanum nitrate, citric acid and/or calcium nitrate were dissolved in deionised water and heated at 100ºC overnight in an oven to dryness, then calcined for an hour at different temperatures (400°C, 600°C and 800°C) for samples where x = 0, and at 800°C for samples with x = 4%, 10%, 16% and 20%. Pictures of the unsubstituted and substituted $LaFeO_3$ are shown in Figures 3 and 4 respectively.



Figure 3: $LaFeO_3$ after being heated at 100 ºC overnight



Figure 4: $La_{1-x}Ca_xFeO_3$ (x = 4%, 10%, 16% and 20%) after being heated at 100 ºC.

4.3 Preparation of Au Catalysts

Au-perovskites were prepared by the single step borohydride method [3]. The support was suspended in distilled water (200 ml) and stirred vigorously. The required amount of diluted $HAuCl_4$ solution (10^{-2} mol/dm^3) was slowly added with continuous stirring. The pH of the solution was maintained at 8.5 by adding 12.5% NH_4OH drop wise under the same conditions. The precipitated solution was aged for 2 h. A solution of $NaBH_4$ prepared in ice water was added rapidly in the required amount to ensure the complete reduction of Au^{3+} to Au^0. The suspended solution was then aged for a further 2 h, filtered and oven-heated for 4 h in an air current at 120ºC.

4.4 Activity Measurements

Catalytic activity was measured using a fixed bed flow reactor as shown in Figure 5. 100 mg of undiluted catalyst was pretreated in a Pyrex glass tube at 300ºC for 2 h in a stream of oxygen (10% oxygen, balance He) at a flow rate of 40 ml/min, then cooled to room temperature still under a flow of oxygen. The reacting gas mixture containing 5% CO, 10% O_2 and 85% He, was admitted at a flow rate of 40 ml/min through the catalyst-bed in the reactor, whilst increasing the temperature from room temperature to 100ºC. Stability measurements were determined by testing the catalyst sample at a constant temperature of 70ºC overnight. The gas flow was controlled by a set of mass flow controllers and the exit gases from the reactor analyzed by gas chromatography (5710A GC, Hewlett Packard).

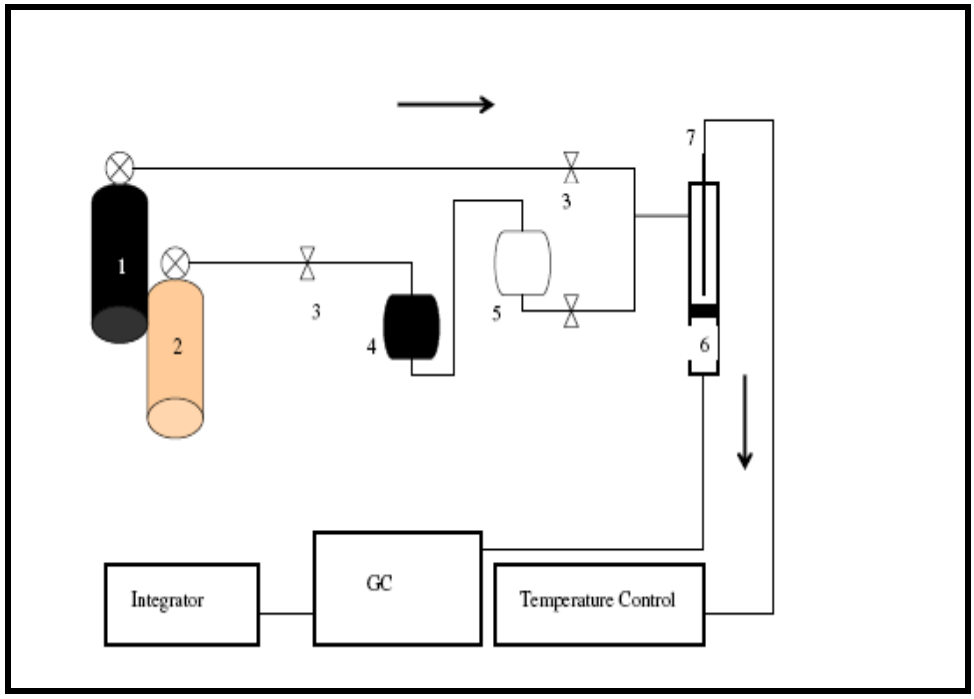


Figure 5: Schematic representation of a reactor used for CO oxidation.

1 – O_2 cylinder
2 – CO cylinder
3 – Shut-off valves
4 – Activated carbon trap to absorb moisture
5 – NaOH trap to absorb CO_2
6 – Reactor and catalyst bed
7 – Thermocouple

4.5 Characterization

4.5.1 BET surface area determination

The surface area of the catalysts was determined using a Micromeritics ASAP 2010 porosimeter. The sample was placed in the sample holder and degassed by passing nitrogen over the catalyst, while being heated at 150°C for 4 h to remove any volatile materials, then allowed to cool to room temperature. The sample was then removed from the degassing port to the analysis port where it was dosed with nitrogen gas at liquid nitrogen temperature. The amount of the adsorbed nitrogen was then used to determine the surface area of the sample.

4.5.2 X-ray powder diffraction

Powder X-ray diffraction data were collected via a Bruker AXS D8 diffractometer using Cu-Kα radiation (40 kV, 40 mA) equipped with a primary beam Gobel mirror, a radial Soller slit, and a Vantec-1 detector. Data were collected in the 2θ range of 5 to 90° in 0.021° steps, using a scan speed resulting in an equivalent counting time of 14.7 s per step.

4.5.3 Raman spectroscopy

Raman spectra were acquired with a Jobin-Yvon T64000 Raman spectrometer operated in single spectrograph mode. Excitation was by means of the 514.5 nm line of an argon ion laser. It was focused onto the sample via an Olympus microscope attachment and the collected light was dispersed onto a charge coupled device (CCD) camera with an 1800 line/mm grating cooled with liquid nitrogen.

For the $AuCaTiO_3$ samples, a 20x objective lens was used, while for the $LaFeO_3$ samples a 50x objective lens was used. Laser power at the sample was kept to ~1.2 mW to prevent localized heating. Data was collected with Lab Spec 4.18 software and acquisition times varied from 120 sec to 180 sec.

4.5.4 X-ray photoelectron spectroscopy

X–ray photoelectron spectra were collected on a Kratos Axis Ultra DLD spectrometer using a monochromatic AlK_α X-ray source (75 W) and an analyser pass energy of 160 eV for survey spectra and 40 eV for detailed scans. Samples were mounted using double-sided adhesive tape, and binding energies referenced to the C (1s) binding energy of adventitious carbon contamination, taken to be 284.7 eV. Data were analyzed using commercial software (CasaXPS; Neil Fairley) and software developed in-house at Cardiff University.

4.6 Calculations

$$\%\ \text{CO conversion} = \left[\frac{CO_{in} - CO_{out}}{CO_{in}}\right] x100$$

where:

CO_{in} = peak area of CO on chromatogram for the reactor inlet gas

CO_{out} = peak area of CO on chromatogram for the reactor outlet gas

4.7 References

1. D.V. Bavykin, A.A. Lapkin, P.K. Plucinki, L. Torrente-Murciano, J.M. Friedrich and F.C. Walsh, *Top. Catal.*, **39** (2006) 151.
2. S. Navale, V. Samuel and V. Ravi, *Bull. Mater. Sci.*, **28** (2005) 391.
3. K. Mallick and M.S. Scurrell, *Appl. Catal. A: Gen.*, **253** (2003) 527.

CHAPTER 5

5 CATALYSTS BASED ON CALCIUM-TITANIUM PEROVSKITES

The mineral $CaTiO_3$ is the founder father of the perovskite structure family [1]. It is widely used in electronic ceramic materials and for immobilizing radioactive waste. TiO_2 has been studied widely for CO oxidation and has shown good results. Thus, the activity of a titania-based perovskite was of great interest in this dissertation.

Other systems that were investigated included gold supported on $LaFeO_3$, $LaMnO_3$, $LaCoO_3$ and $LaCuO_3$ perovskites. Table 7 shows preliminary results of the activity tests of these systems. Only catalysts supported on $CaTiO_3$ and $LaFeO_3$ showed activity below 100°C for which reason the other perovskites (i.e. $LaMnO_3$, $LaCoO_3$ and $LaCuO_3$) were eliminated from the study.

This chapter therefore presents the CO activity and characterisation results for the Au-$CaTiO_3$ catalysts. Chapter 6 will cover Au-$LaFeO_3$ catalysts while Chapter 7 will deal with Au-$La_{(1-x)}Ca_xFeO_3$, where La is substituted with Ca. These systems showed some promising activity.

Table 7: Activity measurements for the different gold-supported perovskites

Catalyst	Calcination Temperature (°C)	BET surface area (m^2/g)	Activity below 100°C
Au-$CaTiO_3$	None	45.1	Active
	400	41.7	Active
	600	34.4	Active
	800	10.1	Active
Au-$LaFeO_3$	400	14.2	Active
	600	19.3	Active
	800	25.4	Active
Au-$LaMnO_3$	400	-	Not active
	600	-	Not active
	800	-	Not active
Au-$LaCoO_3$	400	17.4	Not active
	600	7.40	Not active
	800	11.7	Not active
Au-$LaCuO_3$	400	-	Not active
	600	-	Not active
	800	-	Not active

5.1 Activity and Stability Measurements for Au-$CaTiO_3$

Au-$CaTiO_3$ (100 mg) was tested for CO conversion by flowing the reaction gases over the catalyst at a total flow rate of 40 ml/min. The activity results were recorded at 10°C intervals increasing from room temperature to 100°C. To determine the stability of the catalyst, the results were collected every 30 min at 70°C over 24 h.

5.1.1 Activity Tests

Table 8 and Figure 6 show the activity measurements for Au-$CaTiO_3$ towards CO oxidation at atmospheric pressure as a function of both reaction and calcination temperature. The activity of the catalysts between 30° and 100°C was comparable between catalysts with the support not calcined and those with the support calcined at 400°C. Increasing the calcination temperature of the support to 600°C improved the activity, but a further increase to 800°C resulted in an inactive catalyst. Therefore calcination at 600°C gave the most active catalyst and was considered the optimum temperature for these systems.

*Table 8: Activity measurements for Au-$CaTiO_3$ catalysts**

Reaction Temp°C	**CO conversion (%)**		
	Oven dried	**Calcination Temp°C**	
	NC #	**400°C**	**600°C**
30	10	11	13
40	15	12	18
50	17	16	25
60	20	19	28
70	24	22	40
80	28	26	46
90	30	31	54
100	35	40	66

*Activity as expressed by % CO converted
NC meaning no support calcination, oven dried at 100°C overnight.

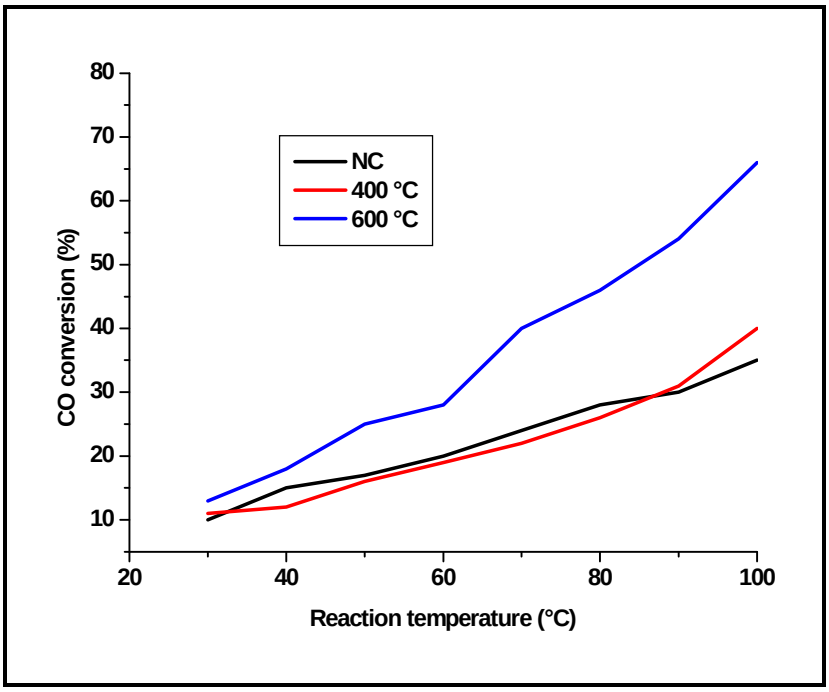


Figure 6: CO conversion over Au-$CaTiO_3$ catalysts

5.1.2 Stability Tests

From the stability tests, high catalytic activity was observed initially for all catalysts, but they deactivated over time on stream. This could be due to reduction of cationic gold probably arising from the Au-perovskite interaction. The catalyst with the support not calcined was very unstable. For example, after 9 h on line there were appreciable drops in activity from 28% to 22% within an hour. The catalyst with the support calcined at 600ºC was more stable than all the other catalysts prepared. Table 9 and Figure 7 show the stability measurements for Au-$CaTiO_3$ towards CO oxidation at atmospheric pressure as a function of time.

*Table 9: Stability measurements for Au-$CaTiO_3$ catalysts**

Time (h)	CO conversion (%)		
	Oven dried	Calcination Temp°C	
	NC #	400ºC	600ºC
1	33	25	33
2	31	22	28
3	30	22	28
4	31	22	27
5	29	21	27
6	29	20	27
7	28	20	27
8	28	21	26
9	28	21	27
10	22	19	26
11	23	19	25
12	22	20	25
13	21	20	25
14	20	20	26
15	19	20	26
16	19	20	25
17	19	20	25
18	19	18	25
19	18	17	23
20	19	17	24
21	19	17	23

*Activity as expressed by % CO converted
NC meaning no support calcination, oven dried at 100°C overnight.

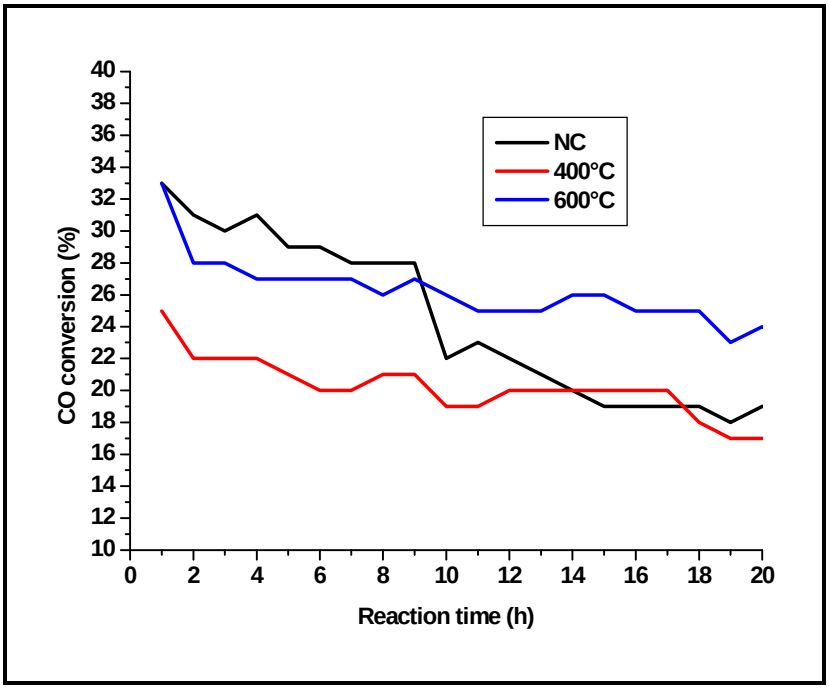


Figure 7: Stability tests for Au-$CaTiO_3$ catalysts

5.2 Characterisation Results for Au-$CaTiO_3$

Characterisation plays a crucial role in understanding the interaction between the support and the metal nanoparticles, and this should lead to a better understanding of the reasons for the increase or decrease in activity. The supports and catalysts were characterized by BET surface analysis, powder-XRD, XPS, XRF, and Raman spectroscopy. The characterization results are discussed below.

5.2.1 BET surface area

There are different variables that play a role in catalyst activity and the surface area is one of those variables. It is reported in literature that the higher the surface area, the more active the catalyst would be [2]. Perovskites have been reported to have surface areas that are less than 10 m^2/g depending on the method of preparation [3].

The citrate method has been reported to give reasonable surface areas [4] and this was our method of choice for the support preparation. In the $CaTiO_3$ system, the support that was not calcined had the highest surface area and as the calcination temperature was increased, the surface area was observed to decrease as shown in Table 10, with 800°C having the lowest surface area of approximately 10 m^2/g.

Table 10: BET Surface area results for $CaTiO_3$ calcined at different temperatures

Catalyst	**Calcination Temperature**	**Surface area (m^2/g)**
$CaTiO_3$	Oven dried at 100°C	45.1
	400°C	41.7
	600°C	34.4
	800°C	10.1

5.2.2 X-ray diffraction

From XRD results, the interested was to establish the phase transformations, new phases to the perovskite pattern, peak shifts and peak broadening. From Figure 8, the expected $CaTiO_3$ XRD pattern was observed which means the prepared perovskite was pure. Apparently, calcination of the support did not change the structure of the perovskite, and no peak shifts or peak broadening was observed with increasing temperature. Loading of gold on the support showed no change in the XRD pattern of the perovskite and the gold peaks could not be detected as they overlapped with the support peaks. The 1wt% Au loading was low.

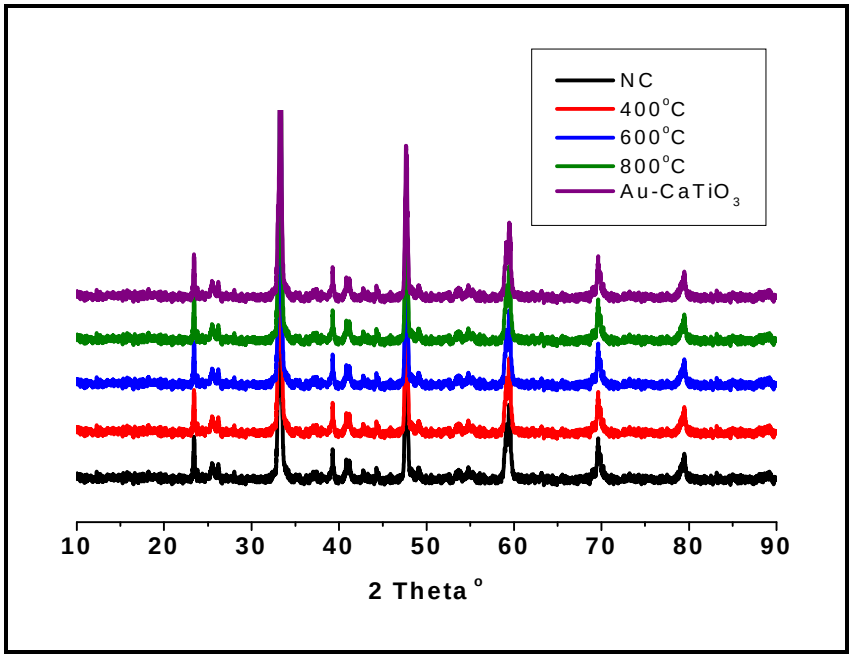


Figure 8: Diffractograms for $CaTiO_3$ calcined at different temperatures

5.2.3 Raman spectroscopy

Raman spectroscopy was used to study the crystallinity of the materials by looking at peak height and peak broadening of characteristic absorptions. It is reported in literature that amorphous materials show broad Raman peaks [5]. Figure 9 shows the observed spectra and the assignments of the peaks are given in Table 11. The supports calcined at 400°C and 600°C were observed to be more crystalline as their peaks were more pronounced and with higher intensity.

Table 11: Symmetry assignments for the observed Raman spectra for $CaTiO_3$

Raman shifts (cm^{-1})	**Assignments**
142	P_1 Raman mode which is related to $CaTiO_3$ lattice mode.
241	P_4 which is the O – Ti – O bending mode.
467	P_7 which is ascribed to the torsional mode.

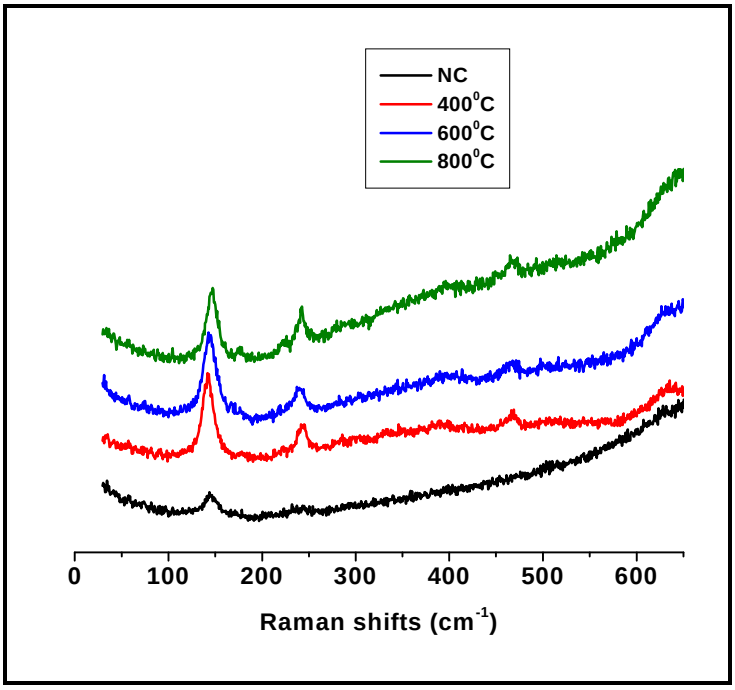


Figure 9: Raman spectra for $CaTiO_3$ calcined at different temperatures

5.2.4 X-ray photoelectron spectroscopy

Surface analysis is very important in evaluating heterogeneous catalysts and the catalysts were therefore analyzed by XPS to determine shifts in binding energies and changes in peak intensities. From Table 12, the catalyst with the support calcined at 600°C had the lowest surface oxygen and the highest titanium content, which led to the system with the best performance in activity. In Figure 10, it can be seen that the intensity of the Au (4f) peaks decreased as the calcination temperature was increased. Also, there was a slight shift to higher binding energies with an increase in calcination temperature.

Table 12: Surface compositions for Au-$CaTiO_3$ by XPS

Calcination Temp^{o}C	Composition %				Elemental ratios	
	O	Ti	Ca	Au	O/(Ti+Ca)	Au/Ti
NC	60.7	14.9	21.5	2.9	1.67	0.19
400	64.5	17.6	17.3	0.6	1.85	0.03
600	58.7	24.5	16.2	0.6	1.44	0.02
800	65.0	18.2	16.4	0.5	1.88	0.03

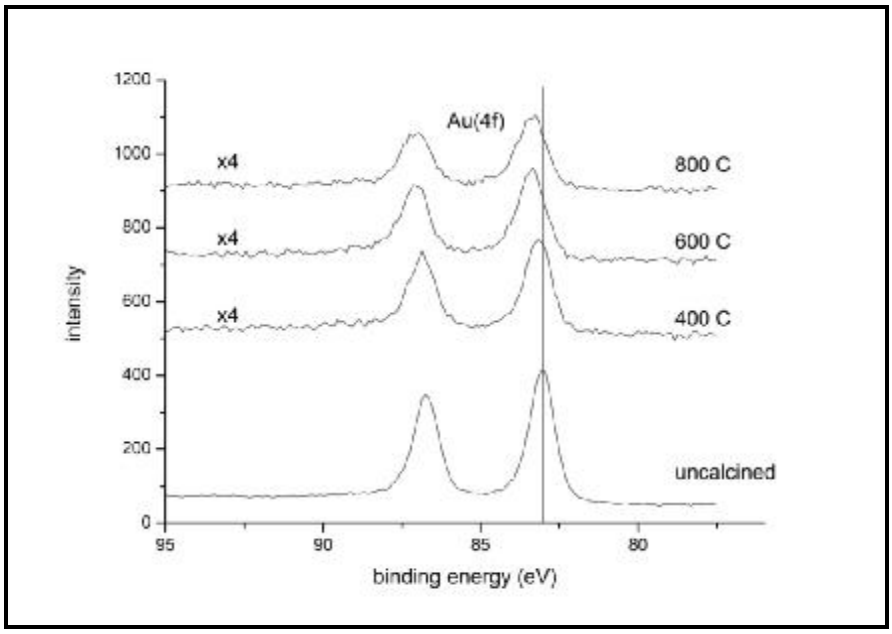


Figure 10: Spectra showing Au (4f) binding energies for Au-$CaTiO_3$

In Figure 11, no significant effect on the Ca (2p) binding energies was noted for all the supports prepared as a result of increasing the calcination temperature. The spectra for O (1s) in Figure 12 show shifts to higher binding energies for the support calcined at higher temperatures.

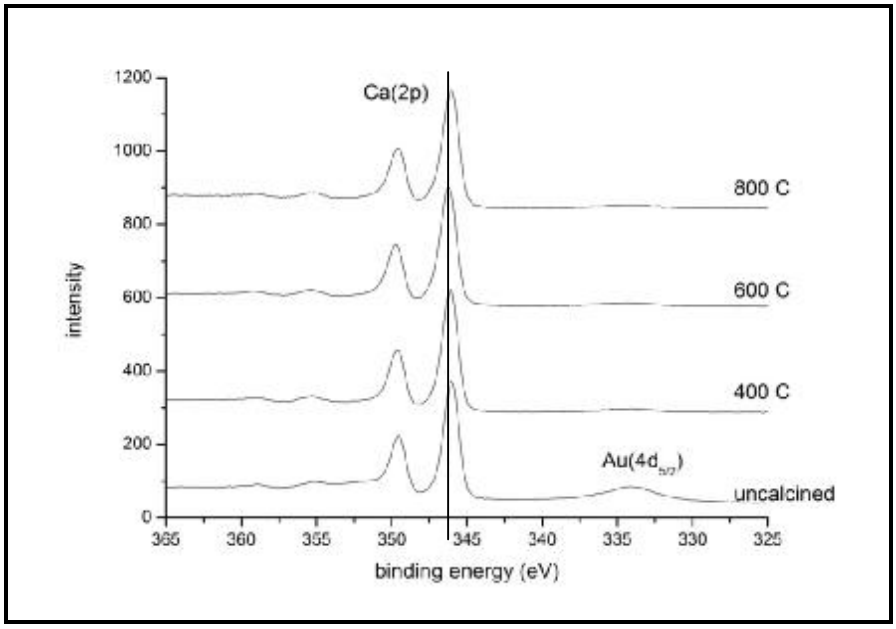


Figure 11: Spectra for Au-$CaTiO_3$ showing the Ca (2p) binding energies

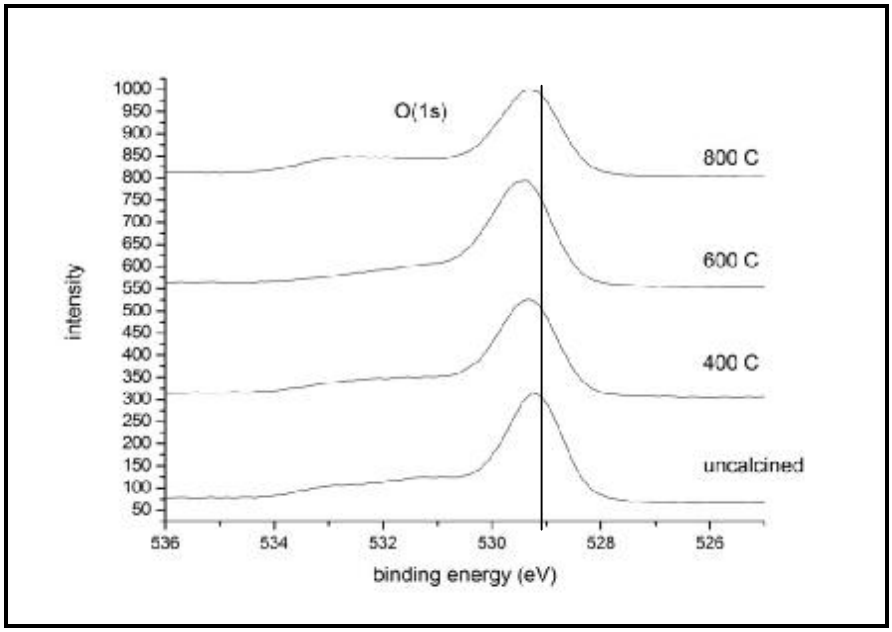


Figure 12: The spectra showing the O (1s) binding energies for Au-$CaTiO_3$

5.3 Discussion

$CaTiO_3$ has been used for the treatment of radioactive wastes and $CaTiO_3$ based perovskites have been used as catalysts for partial oxidation of light hydrocarbons [6]. This perovskite, however, has never been investigated for CO oxidation and the fact that it is titania-based was of interest. The effect of gold loading on $CaTiO_3$ has also never been explored.

Under our test conditions, pure $CaTiO_3$ was not active for CO oxidation. The catalyst with the support calcined at 800°C showed no activity for CO oxidation as well. From surface area analysis, the support calcined at 800°C had the lowest surface area and Raman spectra showed that this support was amorphous. The catalyst with the support calcined at 600°C was the most active and stable in this series of catalysts. This support had reasonable surface area, and it was highly crystalline as shown by Raman spectra.

XPS (Figure 10) analysis of Au- $CaTiO_3$ showed a decrease of the Au (4f) peak as the calcination temperature was increased to 800°C. This could be due to the incorporation of Au into the perovskite structure, and this should lead to better interaction between Au and the support. It was thus expected that the catalyst calcined at 800°C should be more active. However, experiments revealed that this sample did not have any activity.

It was then clear that other factors play a role in the catalyst activity for this system. Calcination temperature plays a vital role in determining the surface area, crystallinity and interaction between the metal and the support. The optimum calcination temperature was presumed to be 600°C. XPS results depicted in Table 11, showed that the catalyst with the support calcined 600°C had the lowest surface oxygen and highest titanium content. It therefore gave the lowest O:(Ti+Ca) ratio and Au:Ti ratio.

This suggests that the Ti^{4+} exerts a strong attraction towards the few surface oxygen atoms remaining. There is also a strong interaction between Au and Ti as the binding energies are observed to shift towards the higher energy as the calcination temperature is increased.

These strong attractive forces seem to enhance the higher catalytic activity observed in the material calcined at 600°C. Higher calcination temperature at, for example, 800°C causes re-oxidation that increases surface oxygen content significantly thereby lowering the interaction, and leads to no catalytic activity.

Overall, the catalyst activity for the gold loaded samples was observed to increase with increasing reaction temperature but gradually deactivated over the period of time investigated. Thus in 5 h, there was ± 8 % decrease in activity.

5.4 References

1. V.V. Lemanov, A.V. Stotnikov, E.P. Smirnova, M. Weihnacht, and R. Kunze, *Solid State Comm.*, **110** (1999) 611.
2. M. Jia, Y. Shen, C. Li, Z. Bao and S. Sheng, *Catal. Lett.*, **99** (2005) 235
3. P. Ciambelli, S. Cimino, G. Lasorella, S. de Rossi, L. Lisi, M. Faticanti, G. Minelli and P. Porta, *Appl. Catal. B: Environ.*, **37** (2002) 231.
4. S. Navale, V. Samuel, V. Ravi, *Bull. Mater. Sci.*, **28** (2005) 391.
5. T. Ivanova, K.A. Gesheva, A. Szekeres, *J. Solid State Electrochem.*, **7** (2002) 21.
6. T. Hayakawa, A.G. Andersen, M. Shimizu, K. Suzuki, K. Takehira, *Catal. Lett.*, **22** (1993) 307.

CHAPTER 6

6 CATALYSTS BASED ON LANTHANUM-IRON PEROVSKITES

$LaFeO_3$ is one of the perovskite-type oxides that have been used as an oxidation catalyst [1]. $LaFeO_3$ is reported to be active in reactions such as propane oxidation, methane combustion and high temperature CO oxidation. Barbero *et al*. [2] and Ciambelli *et al*. [3] did a detailed study on this perovskite for total oxidation of VOCs (volatile organic compounds). Their results were interesting and initiated the investigation of this perovskite for low temperature CO oxidation with an interest in the effect of gold loading. This chapter summarises the activity, stability tests and characterization results of the $LaFeO_3$ system.

6.1 Activity Measurements for Au-$LaFeO_3$

Au-$LaFeO_3$ (0.1 g) was tested for CO conversion in a reaction mixture of 5% CO, 10% O_2 and 85% He at a total flow rate of 40 ml/min. The activity results were recorded at 10°C intervals, increasing the temperature from room temperature to 100°C. To determine the stability of the catalyst, the results were collected every 30 min whilst holding the reaction temperature at 70°C over 24 h.

6.1.1 Activity Tests

Table 13 show the activity measurements for Au-$LaFeO_3$ towards CO oxidation at atmospheric pressure using a total flow rate of 40 ml/min of the reaction gases as a function of temperature. Pure $LaFeO_3$ was not active for CO oxidation under those conditions. Figure 13 is a graphical plot of the results. The catalysts showed an increase in activity with increasing reaction temperature. Calcination of the support seemingly had no effect on the activity of these catalysts as there were insignificant differences between them.

*Table 13: Activity measurements for the Au-$LaFeO_3$ system**

Reaction Temperature ºC	**Calcination Temperature**		
	400ºC	**600ºC**	**800ºC**
	CO conversion (%)		
30	31	25	21
40	40	40	33
50	47	53	48
60	53	62	62
70	79	70	71
80	90	88	84
90	93	90	87
100	95	91	91

* Activity as expressed by % CO converted

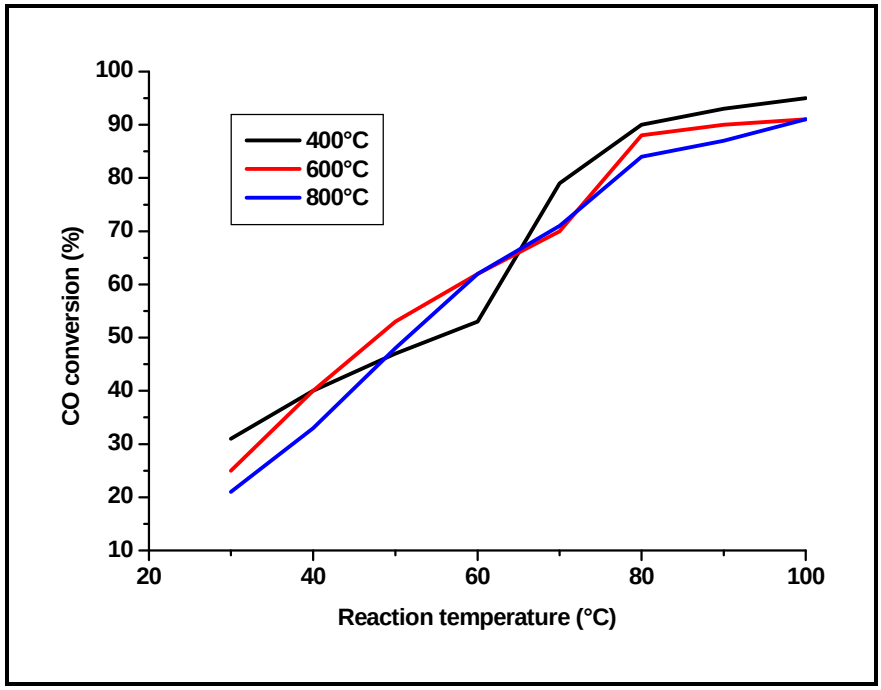


Figure 13: CO conversion over Au-$LaFeO_3$ catalysts

6.1.2 Stability Tests

Table 14 show the stability measurements for Au-$LaFeO_3$ catalysts over 21 h on stream. The catalyst with the support calcined at 400ºC was not stable as it started deactivating after 2 h on stream, see Figure 14. However, after 21 h on stream the 41% conversion is still acceptable, when compared to data for the Au-$CaTiO_3$ catalyst shown in Figure 7. There was an initial increase in activity for the catalysts with supports calcined at 600ºC and 800ºC, probably due to an induction period of about 2 h on stream. The catalysts remained stable throughout the 19 h time on stream. They could be the best catalysts identified in this study for low-temperature CO oxidation.

*Table 14: Stability measurements for Au-$LaFeO_3$ catalysts**

Time (h)	Calcination Temperature		
	400 ºC	**600 ºC**	**800 ºC**
	CO conversion (%)		
1	79	63	77
2	67	93	95
3	67	96	99
4	63	96	94
5	64	96	97
6	63	97	97
7	60	96	99
8	56	96	96
9	63	95	96
10	60	96	96
11	58	95	96
12	57	95	95
13	52	95	97
14	53	96	96
15	52	96	96
16	52	96	96
17	55	96	96
18	52	95	96
19	51	95	96
20	50	97	95
21	41	96	96

* Activity as expressed by % CO converted

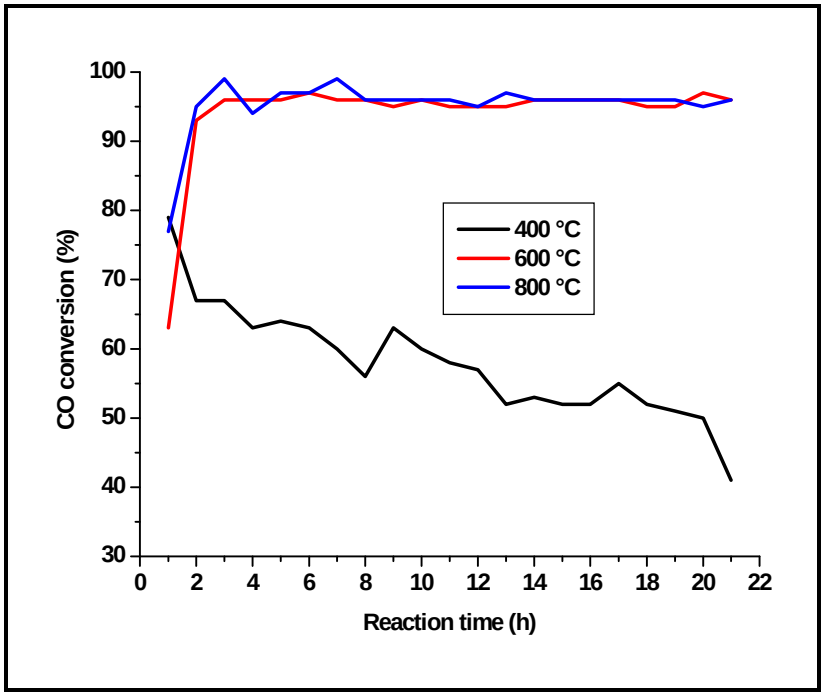


Figure 14: CO conversion for Au-$LaFeO_3$ catalysts

6.2 Characterisation results for Au-$LaFeO_3$

Samples of $LaFeO_3$ support were calcined at various temperatures after which gold was deposited. To understand the effect of calcination and gold loading, these supports and catalysts were characterised by BET surface analysis, powder-XRD, XPS, XRF, and Raman spectroscopy. The results are discussed below.

6.2.1 BET surface area

Table 15 gives the observed surface area results. As the calcination temperature of the support was increased, there was an increase in surface area. The support calcined at 800°C had the highest surface area.

Table 15: Surface area analysis for $LaFeO_3$ calcined at different temperatures

Material	**Calcination Temperature (°C)**	**Surface Area (m^2/g)**
$LaFeO_3$	400	14.2
	600	19.3
	800	25.4

6.2.2 X-ray diffraction

Figure 15 shows the XRD results that were obtained for the calcined supports. The interest was in phase transformations, new phases to the perovskite pattern and peak shifts and peak broadening. From the diffractograms, the expected $LaFeO_3$ pattern was observed, which means that the prepared perovskites were pure. As the calcination temperature of the support was increased there was an increase in the peak intensity that could be due to increased crystallinity. The gold peak however could not be detected as it overlapped with the support peaks and the 1wt% loading was very low.

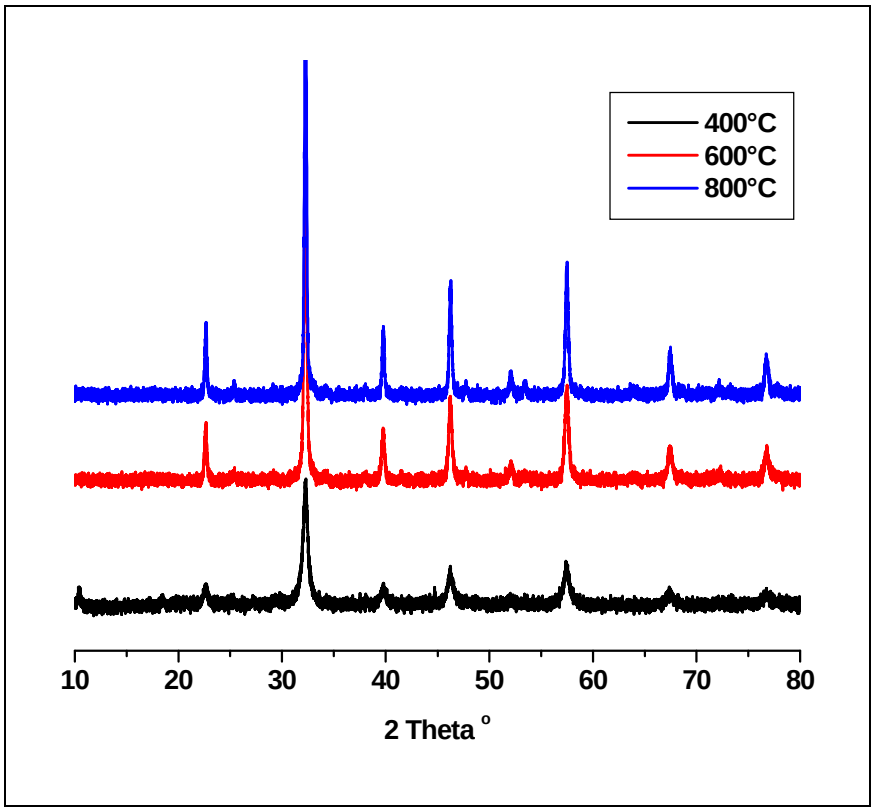


Figure 15: Diffractograms for $LaFeO_3$ systems at various calcination temperatures.

6.2.3 Raman spectroscopy

Little work has been done on the calculation and assignments of the Raman modes for $LaFeO_3$. Moreover, there are some controversial points in the assignments of the modes [4]. For example, the band at ~625 cm^{-1} was assigned to two phonon scattering mode in reference 5 and the same band was assigned to impurity related scattering mode in reference 6. In this work, Raman spectroscopy was used to support the XRD data to determine whether crystallinity plays a role in the activity of these materials by considering the peak intensity and peak broadening.

Very few Raman spectra for $LaFeO_3$ perovskite were found in the literature [4] and they were similar to our observed spectra, see Figure 16. The assignments of peaks found in this spectrum are tabulated in Table 16. The peak intensity increased with an increase in calcination temperature meaning that crystallinity increased when the sample was calcined at higher temperatures.

Table 16: Symmetry assignments for observed Raman peaks for $LaFeO_3$

Raman shifts (cm^{-1})	**Assignments**
431	B_{3g}
628	Two phonon / impurity scattering
991	Two phonon scattering
1129	Two phonon scattering
1306	Two phonon scattering

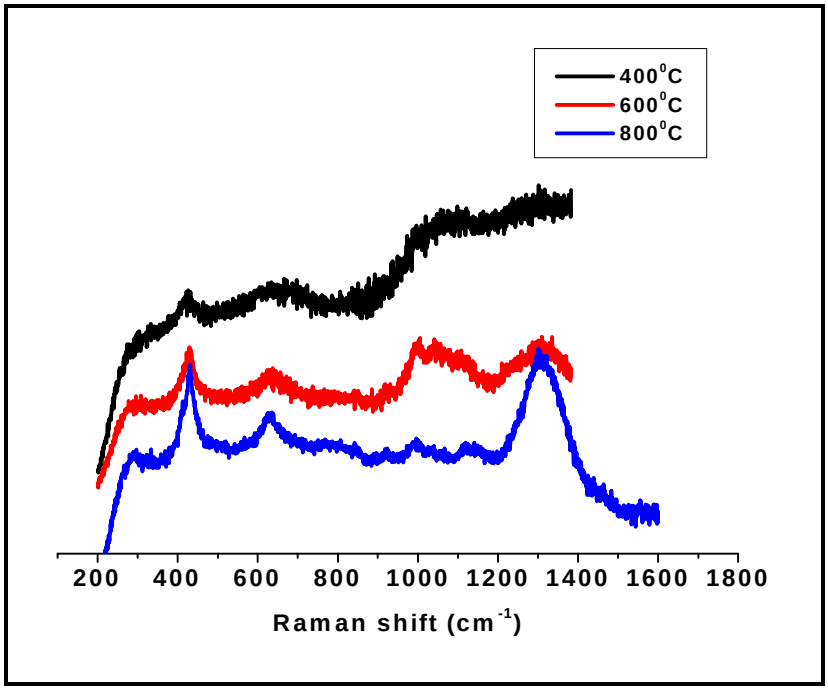


Figure 16: Raman spectra for $LaFeO_3$ at different calcination temperatures

6.2.4 X-ray photoelectron spectroscopy

Catalysts were analyzed by XPS to determine shifts in binding energies in order to determine changes in the atomic interactions. Figures 17 – 20 gives the observed spectra. In Figure 17, there are two doublets corresponding to Au^0 (~ 84.5eV) and Au^{3+} (~ 87eV) species for the Au (4f) transition. Increase in calcination temperature led to an increase in the abundance of the cationic species. There were no shifts in binding energies for all the other spectra as the calcination temperature was increased [Figures 18 – 20]. Quantification of surface compositions of these materials was not feasible due to uncertainty in the La (3d) sensitivity factor for $LaFeO_3$.

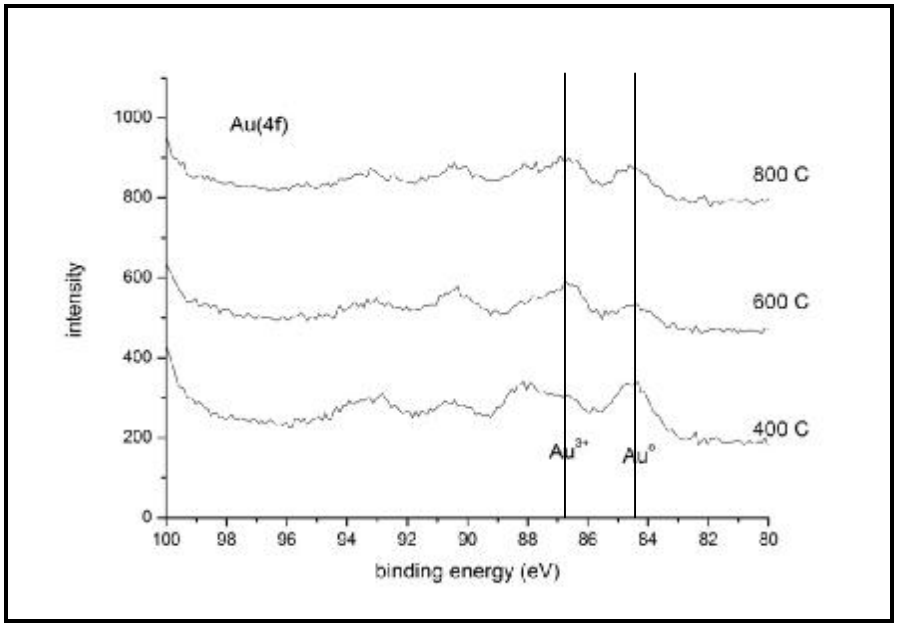


Figure 17: Spectra showing Au (4f) binding energies for Au-$LaFeO_3$

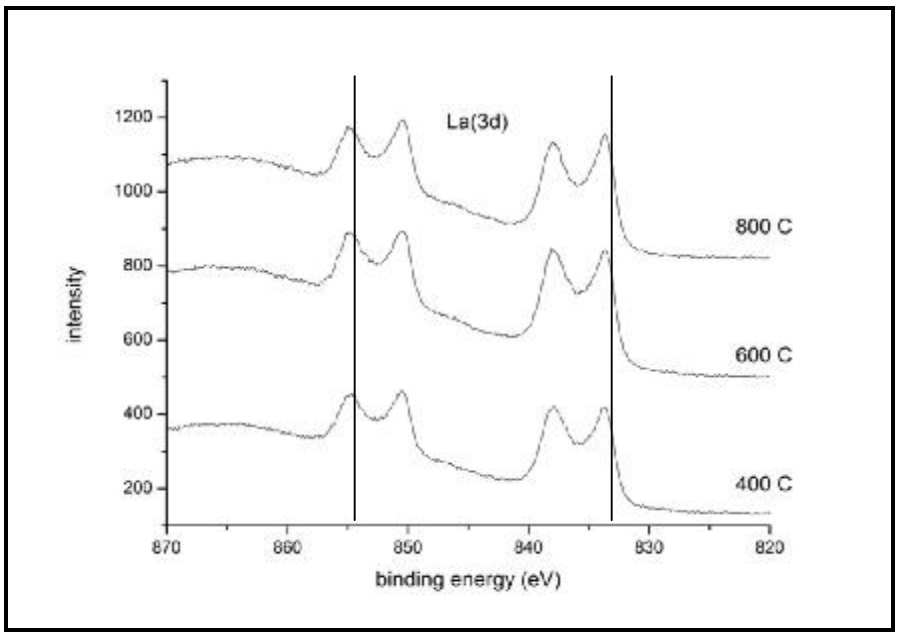


Figure 18: Spectra showing La (3d) binding energies for Au-$LaFeO_3$

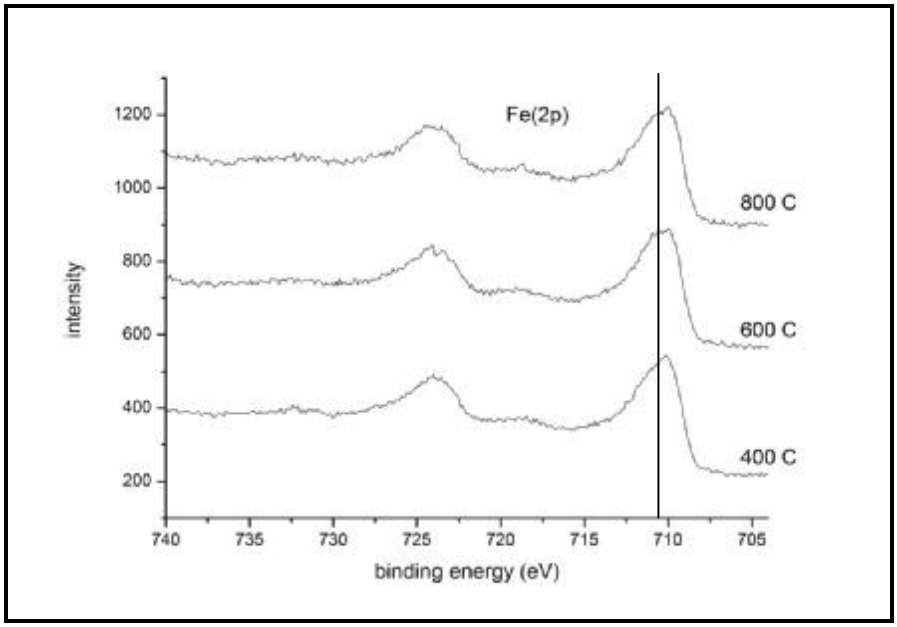


Figure 19: Spectra showing Fe (2p) binding energies for Au-$LaFeO_3$

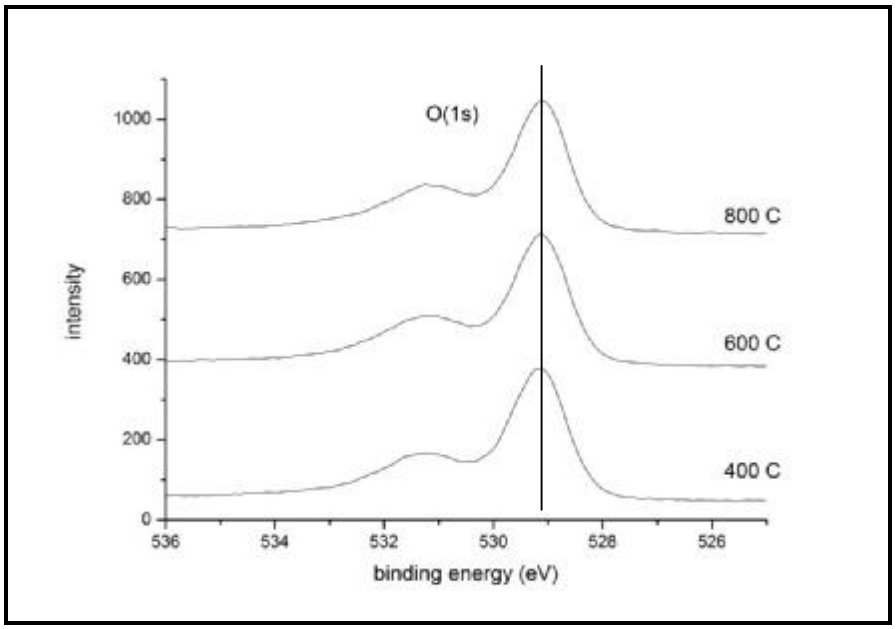


Figure 20: Spectra showing O (1s) binding energies for Au-$LaFeO_3$

6.3 Discussion

$LaFeO_3$ has been investigated for high temperature CO oxidation. For example, a study by Colona *et al.* [7], showed activity at temperatures above 200°C. As expected in our study, $LaFeO_3$ was not active for low temperature CO oxidation. The effect of gold on perovskite for high temperature CO oxidation was investigated by Russo *et al.* [8], and the 2wt% Au-$LaNiO_3$ gave the best results with T_{50} = 156 °C. To investigate the effect of Au loading on low temperature CO oxidation, we prepared the $LaFeO_3$ support at different calcination temperatures.

The supports calcined at 600°C and 800°C had the highest surface area and were more crystalline, and the resulting catalysts were more stable on stream. There was not much difference in the activity of all the Au-$LaFeO_3$ catalysts.

From XRD analysis (Figure 15), the peaks became more pronounced as the calcination temperature was increased, which implies an increase in crystallinity. However, the activity of the different catalysts was similar despite the increase in crystallinity. Therefore, crystallinity does not affect the activity but the stability of these catalysts.

Figure 17 shows a reduction in intensity of the Au(4f) peak as the calcination temperature of the support was increased. This is thought to relate to the incorporation of the cationic species into the support. The $LaFeO_3$ system showed interesting results for CO oxidation and with improvement could be one of the best systems for the reaction of interest. Calcination of the support at higher temperatures was found to play a crucial role in the stability of these materials with time on stream.

6.4 References

1. N. Yamazoe and Y. Teraoka, *Catal. Today*, **8** (1990) 175.
2. B.P. Barbero, J.A. Gamboa and L.E. Cadùs, *Appl. Catal. B: Environ.,* **65** (2006) 21.
3. P. Ciambelli, S. Cimino, S. de Rossi, L. Lisi, G. Minelli, P. Porta and G. Russo, *Appl. Catal. B: Environ*., **29** (2001) 239.
4. Y. Wang, J. Zhu, L. Zhang, X. Yang, L. Lu and X. Wang, *Mater. Matt.*, **60** (2006) 1767.
5. N. Koshizuka, S. Ushioda, *Phys. Rev., B*, **22** (1980) 5394.
6. S. Venugopalan, M. M. Becker, *J. Chem. Phys.*, **93** (1990) 3833.
7. S. Colona, S. De Rossi, M. Faticanti, I. Pettiti and P. Porta, *J. Mol. Catal. A*, **187** (2002) 269.
8. N. Russo, D. Fino, G. Saracco and V. Specchia, *Catal. Today*, **137** (2008) 306.

CHAPTER 7

7 CATALYSTS ON SUBSTITUTED LANTHANUM-IRON PEROVSKITES

The effect of partial substitution of either the A or B sites and sometimes both sites has been reported to result in structural defects such as anionic or cationic vacancies that produce highly stable and active perovskites [1]. In Chapter 6, the Au-$LaFeO_3$ catalyst was shown to give the most promising results and calcination at higher temperatures gave the most stable catalyst. Therefore the effect of partial substitution of La (the A-site) with Ca was investigated using the catalyst with the support calcined at 800°C. The activity and stability of the Au-$LaFeO_3$ and Au-$La_{1-x}Ca_xFeO_3$ were compared. This chapter summarises the results obtained.

7.1 Activity Measurements for Au-$La_{1-x}Ca_xFeO_3$

Au-$La_{1-x}Ca_xFeO_3$ (0.1 g) was tested for CO conversion in a reaction mixture of CO, O_2 and balanced He at a total flow rate of 40 ml/min. The activity and stability tests were recorded as explained in section 6.1.

7.1.1 Activity Tests

Table 17 shows the results obtained over Au-$La_{1-x}Ca_xFeO_3$ catalysts (where x = 0, 4%, 10%, 16% and 20%) for CO conversion. The support alone was not active for CO oxidation under these test conditions. Loading gold on the support resulted in an increase in activity as the reaction temperature was increased. Substituting La with 4% calcium had a negative effect on catalyst activity, see Figure 21. Increasing the calcium content to 10% had a positive effect at temperatures above 70°C on stream. However, further increase in calcium content (16% and 20%) resulted in a significant decrease in catalytic activity. Therefore substitution of La by Ca was not beneficial in this system under the test conditions used.

*Table 17: Activity measurements for Au-$La_{1-x}Ca_xFeO_3$**

Temperature (°C)	**CO conversion (%)**				
	Ca = 0%	**Ca = 4%**	**Ca = 10%**	**Ca = 16%**	**Ca = 20%**
30	21	20	14	15	9
40	33	23	28	22	15
50	48	36	35	32	24
60	62	49	55	44	37
70	71	70	71	62	45
80	84	82	90	71	59
90	87	85	95	73	60
100	91	88	96	78	65

*Activity as expressed by % CO converted

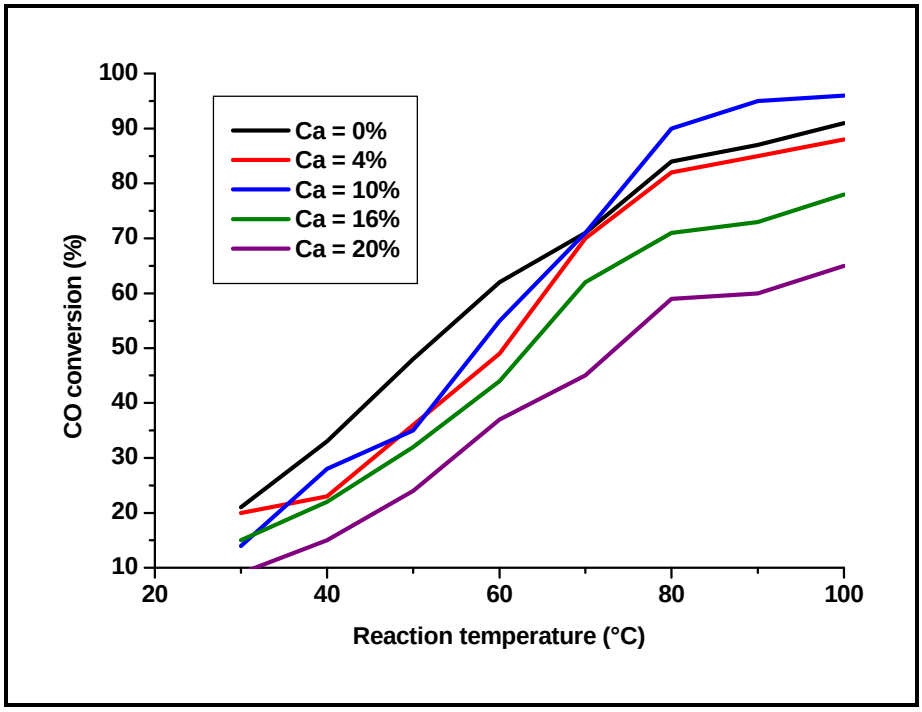


Figure 21: CO conversion over Au-$La_{1-x}Ca_xFeO_3$ at different reaction temperatures

7.1.2 Stability tests

Catalysts stability was determined over 20 h on stream and the results are given in Table 18 and plotted in Figure 22. The catalyst with no calcium had superior activity and stability when compared to all the catalysts substituted with calcium. Generally, at the onset of the reaction, it was observed that a higher calcium loading led to a decrease in activity: except for the 10% Ca. The catalyst substituted with 4% Ca had a higher activity than the 16% Ca, which in turn had a higher activity than the catalyst with 20% Ca. The catalyst with 10% Ca loading gave the best results of all the substituted catalysts but was still not as active as Au-$LaFeO_3$. Overall, substitution of lanthanum by calcium resulted in a decrease in activity and stability when compared to Au-$LaFeO_3$.

*Table 18: Stability measurements for Au-$La_{1-x}Ca_xFeO_3$**

Time (h)	**CO conversion (%)**				
	Ca = 0%	**Ca = 4%**	**Ca = 10%**	**Ca = 16%**	**Ca = 20%**
1	77	26	42	18	4
2	95	57	59	19	4
3	99	63	76	21	4
4	94	61	76	23	7
5	97	60	75	23	8
6	97	58	73	25	14
7	99	56	72	24	17
8	96	56	71	27	18
9	96	55	71	28	21
10	96	54	71	27	24
11	96	54	68	28	24
12	95	53	69	28	24
13	97	51	67	29	27
14	96	49	64	29	27
15	96	51	67	29	25
16	96	50	66	28	29
17	96	48	68	30	31
18	96	52	62	29	33
19	96	51	67	29	32
20	95	51	67	29	32

*Activity as expressed by % CO converted

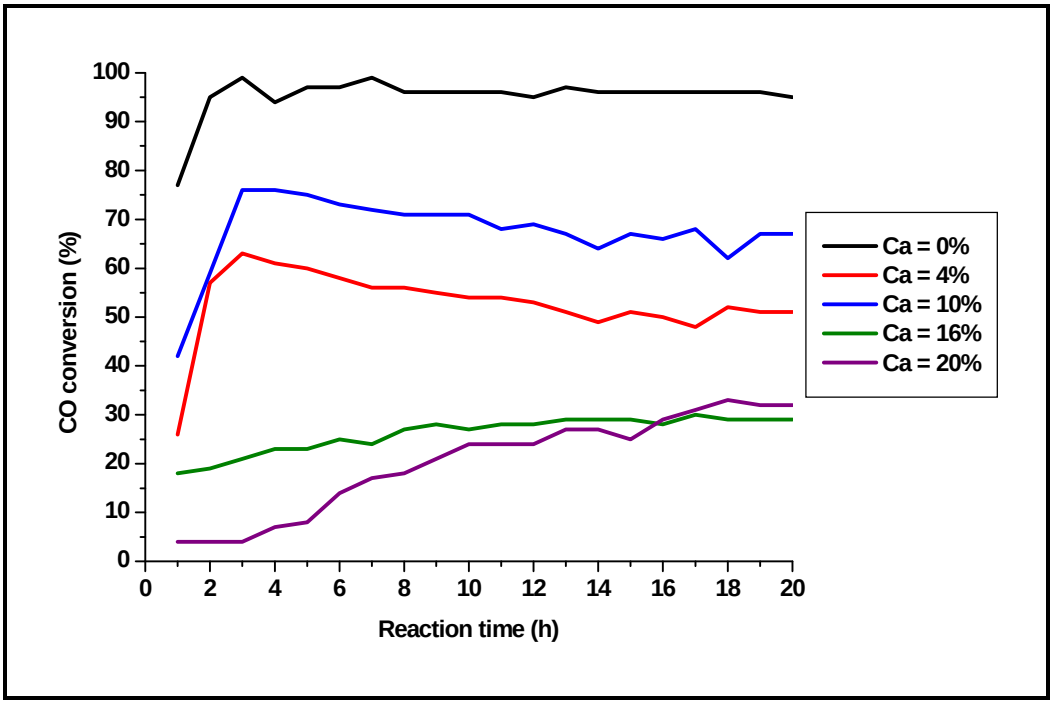


Figure 22: CO conversion over time on stream for Au-$La_{1-x}Ca_xFeO_3$

7.2 Characterisation Results for Au-$La_{1-x}Ca_xFeO_3$

Substitution of La with Ca should bring about changes in the structure of $LaFeO_3$ and the interaction between atoms. To determine these changes alongside the effect of gold on activity, the supports and catalysts were characterised for BET surface area, XRD, XPS, XRF and Raman spectroscopy. The results obtained are discussed below.

7.2.1 BET surface area

Substitution of La with 4%Ca resulted in a decrease in the surface area of the support. Increasing the Ca loading to 10% or 16%, progressively led to a further drop in the surface area. The support with 20% Ca loading, however, had a surface area that was equivalent to the 4 % calcium loaded support, see Table 19.

Table 19: Surface area results for Au-$La_{1-x}Ca_xFeO_3$

Support	**Calcium loading (%)**	**Surface area (m^2/g)**
$La_{1-x}Ca_xFeO_3$	0	25.4
	4	17.5
	10	14.9
	16	14.3
	20	17.5

7.2.2 X-ray diffraction

The different supports were analyzed using powder-XRD to determine the effect of calcium loading on the structure of the perovskite. Figure 23 shows the XRD patterns (2θ values of 10 to 90°), for all the $La_{1-x}Ca_xFeO_3$ perovskites prepared. A decrease in peak intensity was observed with increasing Ca loading. Higher Ca loading especially the 20% loading led to coverage of the perovskites such that the peaks became weak in the XRD pattern. Gold peaks were not visible in the XRD patterns as the 1-wt% Au was below the detection limit.

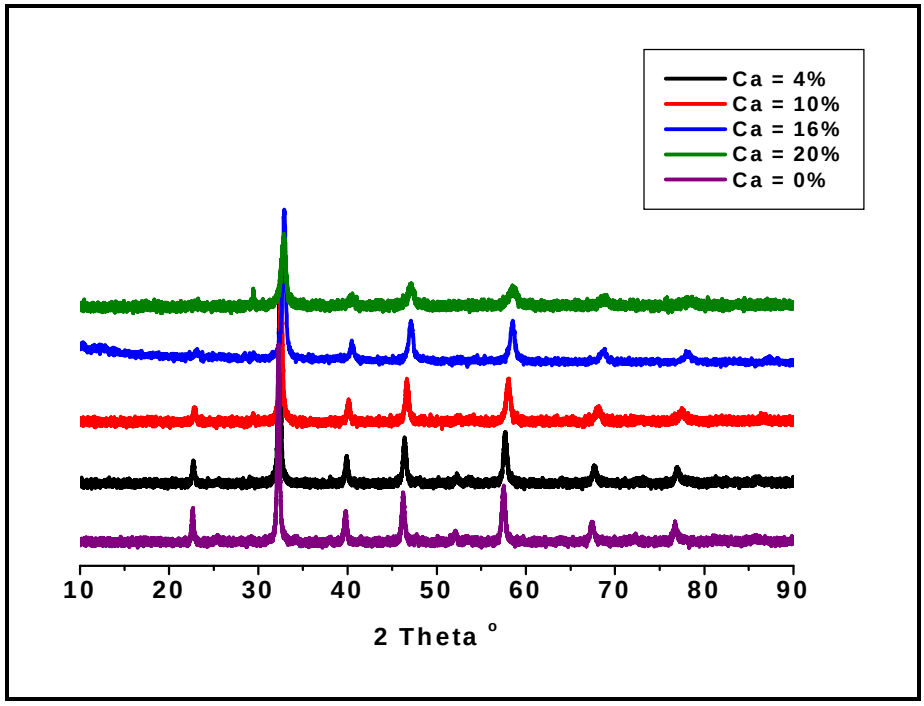


Figure 23: XRD patterns showing the effect of calcium loading on $LaFeO_3$

7.2.3 Raman Spectroscopy

No peaks were observed in the Raman region for all the Ca doped-supports. Therefore, modification of $LaFeO_3$ with Ca decreased the crystallinity of the materials drastically. Our results correspond with what is reported in literature for featureless materials [2].

7.2.4 X- ray photoelectron spectroscopy

The surface analysis results from XPS are given in Figures 24-28. For the 4% calcium loaded catalysts, the presence of cationic gold species (~87eV) and some metallic gold (~84eV) was detected. For the samples substituted with 16% or 20% calcium, the gold signal was not evident, probably because there was no Au on the surface of the support, see Figure 24.

The Ca (2p) spectra in Figure 25 show dramatic differences as a function of Ca loading. The Ca (2p) spectra exhibit two components at ~346eV and ~349eV, both of which increased in relative intensity as the Ca loading increased. The total Ca (2p) intensity increased with Ca loading up to the 16% calcium substitution; the intensities of samples loaded with 16% and 20% calcium were very similar.

Presumably this represents Ca species in two different environments or lattice positions. This conclusion is supported by the La (3d) spectra shown in Figure 26, where the spectra corresponding to 16% and 20% Ca loadings show evidence for two La states in the broadening of the signals, reflecting different interactions between the La and Ca atoms. There were no significant changes in the Fe (2p) binding energies for the Au-$La_{1-x}Ca_xFeO_3$ catalysts as seen in Figure 27.

For the samples substituted with 16% and 20% Ca, there was a large increase in the high binding energy component of the O (1s) spectra compared with the lower Ca loadings, possibly reflecting the contribution from “CaO” species to the O (1s) envelope. This is clearly correlated with the observations made in the Ca (2p) and La (3d) signals concerning different Ca species.

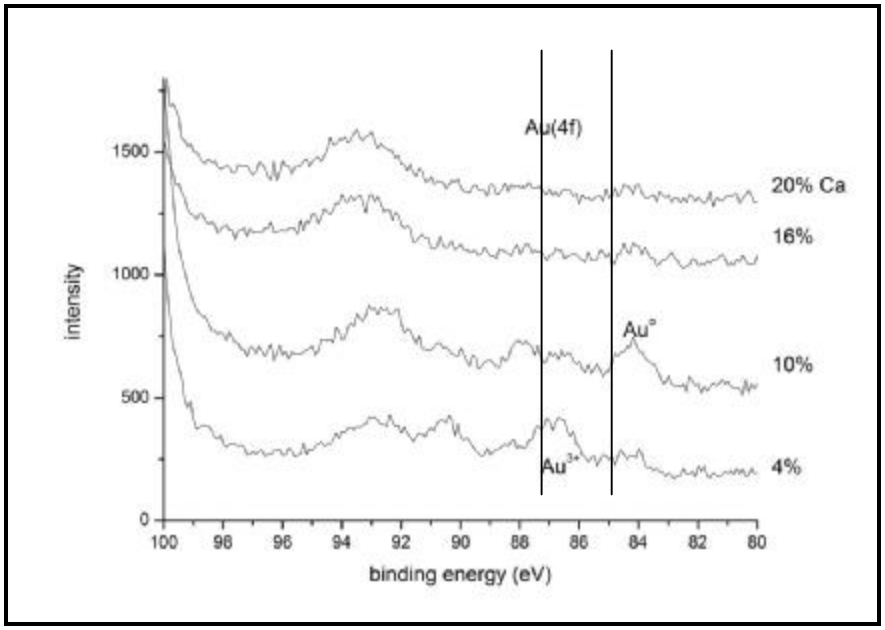


Figure 24: Spectra showing Au (4f) binding energies for Ca doped Au-$LaFeO_3$

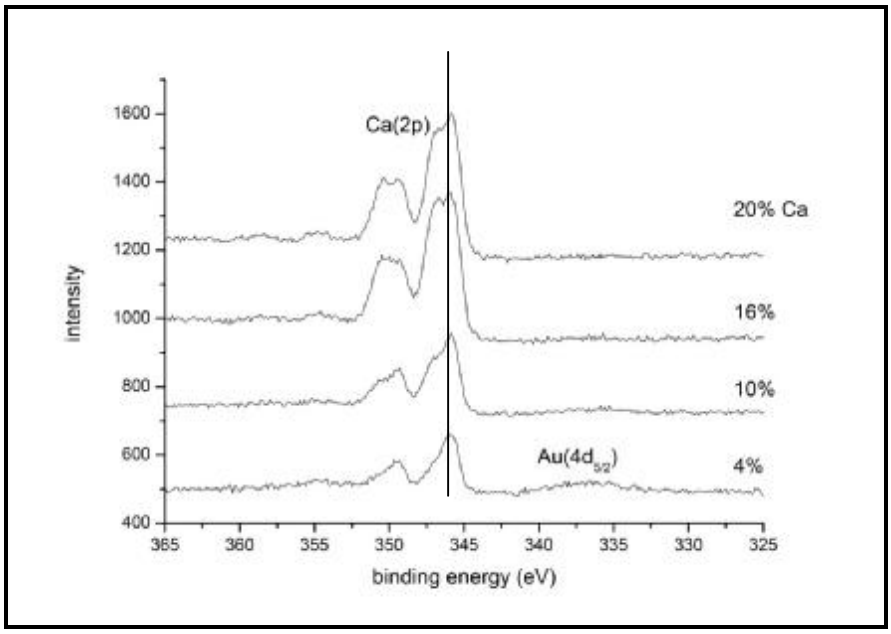


Figure 25: Spectra showing Ca (2p) binding energies for Ca doped Au-$LaFeO_3$

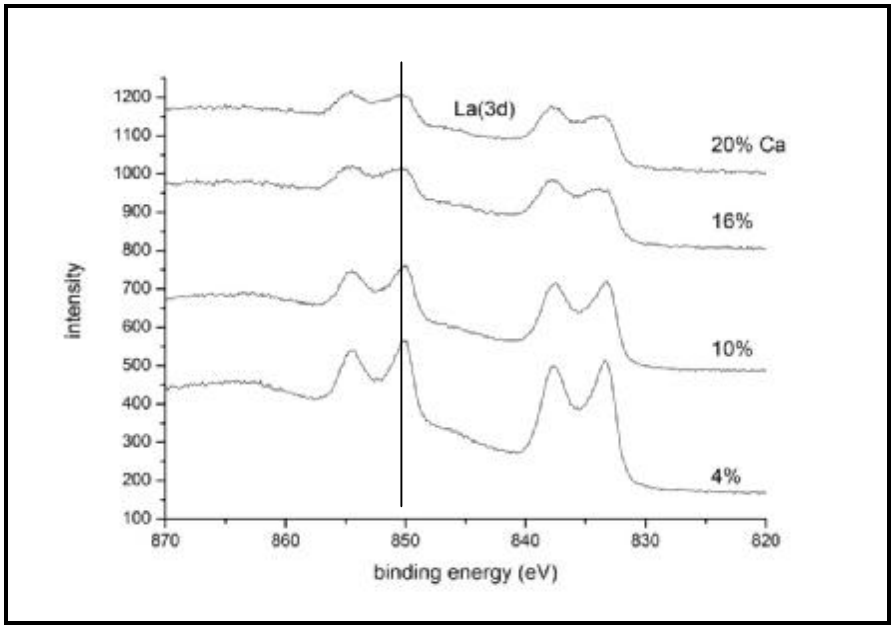


Figure 26: Spectra showing La (3d) binding energies for Ca doped Au-$LaFeO_3$

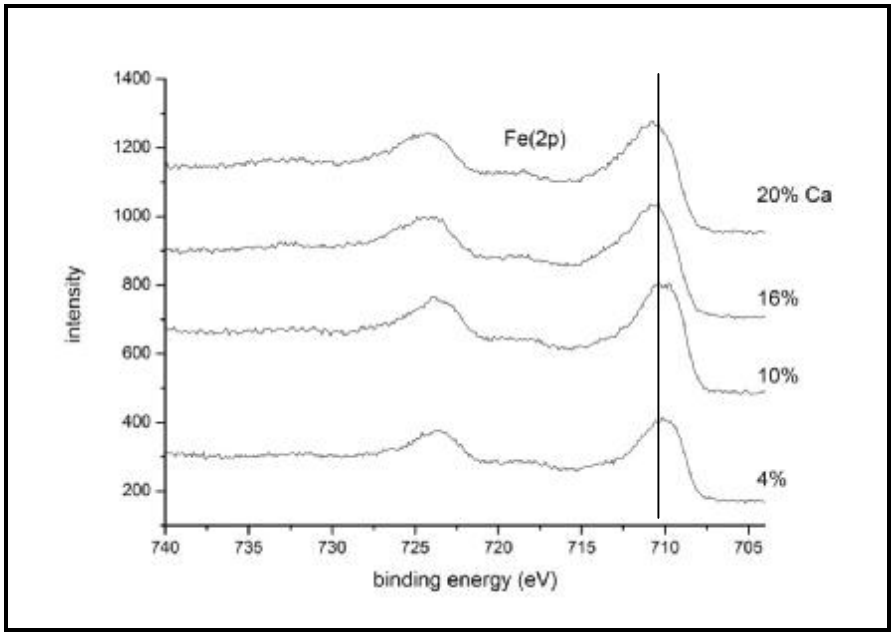


Figure 27: Spectra showing Fe (2p) binding energies for Ca doped Au-$LaFeO_3$

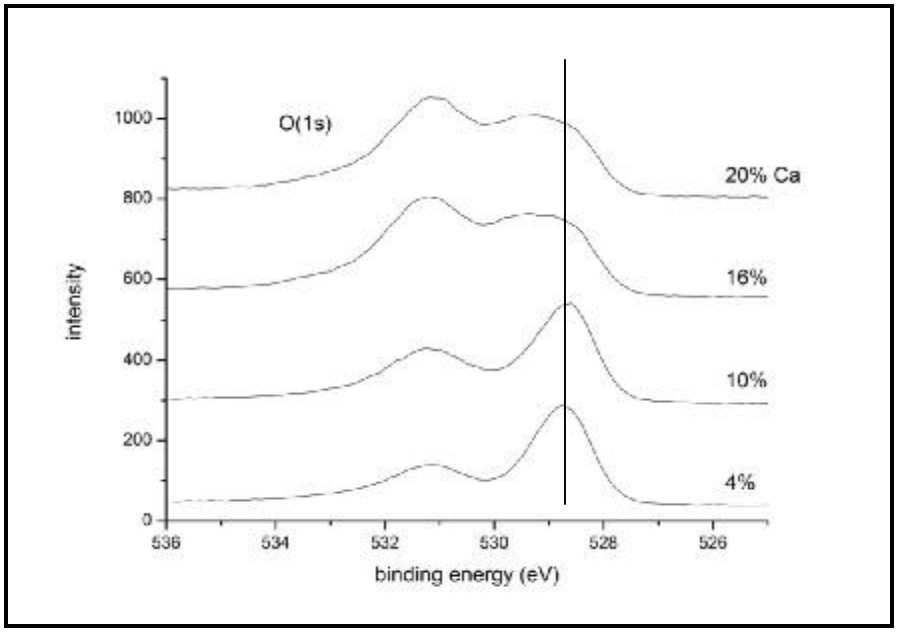


Figure 28: Spectra showing O (1s) binding energies for Ca doped Au-$LaFeO_3$

7.3 Discussion

Substitution of La with transition metal cations has been investigated by different researchers, some showing positive effects and others showing negative effects. Barbero *et al.* [1] observed improved catalytic activity in propane and ethanol combustion using $LaFeO_3$ substituted with different amounts of calcium. Work by Ciambelli *et al.* [3] showed a decrease in catalytic activity with higher magnesium content in $LaFeO_3$ for methane combustion and CO oxidation.

In this study, the $La_{1-x}Ca_xFeO_3$ support was not active for CO oxidation under our reaction conditions. Loading gold onto the support had a positive effect on the activity for CO oxidation. Substituting La with calcium resulted in a decreased catalytic activity.

All the calcium containing samples had lower surface areas: as the calcium loading was increased, the surface area decreased. From XRD analysis (Figure 23), the intensity of the diffraction lines decreased due to the thickening of CaO layer burying the crystalline structure of the perovskite. This was also supported by the analysis from Raman spectroscopy where no bands for the substituted $LaFeO_3$ were observed due the catalysts being amorphous and featureless arising from the presence of CaO.

In Figure 25, there was evidence of calcium being in two different environments resulting in different interactions between lanthanum and calcium. The decrease in surface area, crystallinity and different species of calcium led to a decrease in catalyst activity and stability. Therefore substitution of lanthanum with calcium cannot be accommodated into $LaFeO_3$ perovskite lattice beyond a certain degree of substitution. The optimum calcium substitution was 10%; any further increase in calcium loading resulted in surface coverage instead of lattice substitution.

7.4 References

1. B.P. Barbero, J.A. Gamboa and L.E. Cadùs, *Appl. Catal. B: Environ.*, **65** (2006) 21.
2. T. Ivanova, K.A. Gesheva and A. Szekeres, *J. Solid State Electrochem.*, **7** (2002) 21.
3. P. Ciambelli, S. Cimino, S. de Rossi, L. Lisi, G. Minelli, P. Porta and G. Russo, *Appl. Catal. B*: *Environ.*, **29** (2001) 239.

CHAPTER 8

8 CONCLUSION

Unlike inert bulk gold, supported gold nanoparticles are highly active in many reactions. Their catalytic activity depends especially on the nature of the support, preparation method, calcination temperature, the effect of promoters, and the size of the Au clusters. Various materials have been examined to support nanogold particles for reactions such as CO oxidation. Of these, TiO_2 is extremely active, and on this support, nanogold particles can catalyse the CO oxidation reaction at sub-ambient temperatures as well as catalysing the preferential oxidation of CO in hydrogen rich streams (PROX) at ambient temperatures. An attempt to deposit nanogold particles on perovskites for high temperature CO oxidation has shown improved catalytic activity. However, these systems have not been investigated for low temperature CO oxidation.

Perovskite type-oxides are known to be tolerant to high temperatures and have been found to be active for various reactions. Their high stability allows for partial substitution of either the A or the B site, which results in structural defects, such as anionic or cationic vacancies that can be manipulated to optimize activity and/or stability. One of the drawbacks of perovskites in catalytic investigations is their low surface area (<10 m^2/g). From the BET surface area analysis, the prepared perovskites in this study had surface areas higher than 10 m^2/g. Therefore, the citrate method was successful in synthesising perovskites with reasonable surface areas.

Calcination at different temperatures influenced the surface area and crystallinity of these materials, which in turn affected the catalyst activity. To produce an active Au-based catalyst, the optimum calcination temperature was 600°C for the $CaTiO_3$ support, but for the $LaFeO_3$ support the best support was calcined at 800°C. Therefore, in conclusion, calcination plays a crucial role in the activity of these materials.

In addition, there was evidence of Au being incorporated into the perovskite as the calcination temperature increased. This resulted in better interaction between the Au and the support calcined at the optimum temperature. Calcination temperature therefore enhances the interaction of the metal with the support, which affects the activity of these catalysts.

In this study, addition of promoters like Ca did not improve the catalytic performance but instead depressed activity dramatically as the Ca loading was increased. The assumption is that, instead of Ca inducing changes in the crystalline structure of the perovskites, the CaO added to the perovskites formed an amorphous layer on the perovskite. There was evidence of calcium being in two different environments suggesting different interactions between lanthanum and calcium. Therefore substitution of lanthanum with calcium was achieved up to a certain degree but it was not beneficial in this system.

The Au-$LaFeO_3$ catalyst showed the best results for CO oxidation and was stable. However, Au/perovskites had low conversions at ambient temperature, which was the interest for this study. Pure perovskites investigated in this study were not active under the investigated conditions (low temperature) as expected. The activity of perovskites increased upon gold deposition.

From XPS analysis, it was observed that, in the active catalysts both cationic and metallic gold co-existed, whilst in the inactive catalysts the gold existed predominantly in one of the forms. Further work aimed at improving the activity of Au/perovskites for low temperature CO oxidation would be beneficial seeing that these materials are promising.

In conclusion, the citrate method was successfully used to prepare the different perovskites and the deposition-precipitation method used to deposit gold onto the supports. The calcination temperature at which the support is subjected to prior to Au addition is crucial in preparing the correct support. Correct procedures result in the preparation of catalysts with higher catalytic activity. Overall, perovskites are intrinsically poorer supports than TiO_2, Al_2O_3, ZnO etc. for low temperature CO oxidation but their activity improved upon gold addition. Therefore the presence of gold nanoparticles significantly enhanced the activity of these materials although the support itself is suspected to be involved in the reaction mechanism.